LPS stimulates dynamic changes in B cell metabolism to promote proliferation

Dana M.S. Cheung[1], Momchil Razsolkov[1], Fabrizia Bonacina[2], Stephen Andrews[1], Megan Sumoreeah[1], Linda V. Sinclair[1], Andrew J.M. Howden[1] and J. Simon C. Arthur[1*]

1) Division of Cell Signalling and Immunology, School of Life Sciences, University of Dundee, Dow St, Dundee, DD1

2) Department of Pharmacological and Biomolecular Sciences "Rodolfo Paoletti", University of Milan, via Balzaretti 9, 20133 Milan, Italy

* Corresponding Author. j.s.c.arthur@dundee.ac.uk, Division of Cell Signalling and Immunology, School of Life Sciences, University of Dundee, Dow St, Dundee, DD1

Abstract

Following activation, naïve B cells exit quiescence and enter a proliferative phase before becoming mature antibody-producing or memory B cells. One method of activation is to use Lipopolysaccharide (LPS), a well-established B cell mitogen that can drive proliferation *ex vivo.* Using quantitative proteomics, we identify an upregulation of proteins following LPS stimulation involved in metabolic pathways including amino acid uptake and cholesterol biosynthesis. We highlight the large, neutral amino acid transporter SLC7A5 as a target of LPS-induced activation, and by utilising SLC7A5 conditional knockout mice, we demonstrate the requirement of this transporter for B cell proliferation *ex vivo*. LPS stimulation increased cellular cholesterol levels and inhibition of the rate-limiting enzymes HMG-CoA-reductase (HMGCR) and Squalene monooxygenase in the cholesterol biosynthesis pathway significantly reduced proliferation. The critical role of the cholesterol biosynthetic pathway was not limited to LPS. Stimulation via TLR7, TLR9, CD40 and the B Cell Receptor also increased cholesterol levels and inhibition of HMGCR reduced proliferation. Together these results suggest a common requirement for metabolic rewiring in B cells to allow proliferation in response to activation.

Introduction

B cells form a critical component of the adaptive immune system and are perhaps best known for the production of antibodies. Naïve B cells express IgM and potentially IgD. Following activation, B cells have the potential to switch from IgM to either IgG, IgA or IgE production, depending on the mechanism of activation and cytokine environment [1,2]. Two main classes of activation have been described; T cell-dependent (TD) and T-independent (TI). In TD activation, following recognition of a protein antigen via the B cell receptor (BCR), the B cell can present peptides from the antigen to CD4 T cells, resulting in T cell activation. At the same time, stimulation of CD40 on the B cell via CD154 (CD40L) promotes B cell maturation, including proliferation, class switch recombination (CSR) and somatic hypermutation[3]. This results in the production of high-affinity class-switched antibodies. *In vivo*, T-dependent activation occurs in germinal centres and has been proposed to be the major way in which high-affinity antibodies and B cell memory are generated [4]. In contrast, TI antigens are usually not proteins, with most being polysaccharides and frequently activate B cells via Toll-like receptors (TLRs) potentially in combination with the BCR[1]. Unlike TD antigens, TI antigens are not classically associated with geminal centre formation *in vivo* and are instead associated with the production of low-affinity IgM antibodies [5].

A well-established model to study TI B cell activation *ex vivo* is to use Lipopolysaccharide (LPS), which stimulates TLR4 [6,7] and induces robust B cell proliferation and antibody secretion both *ex vivo* [8,9] and *in vivo*[10]. LPS is a major constituent of the outer membrane of gram-negative bacteria which is composed of three domains: lipid A, the core oligosaccharide, and the O antigen [11]. Upon activation, TLR4 propagates downstream signalling through the adaptor proteins MyD88 and TRIF, which in turn activates pathways including MAPK and NF-κB[12,13]. While this pathway has been most extensively studied in innate immune cells it can also elicit a range of responses, including proliferation and cytokine production in B cells [14]. The essential role of TLR4 in LPS-induced activation of B cells has been demonstrated by studies using TLR4-deficient mice. In contrast to B cells from wild-type mice, B cells from TLR4 knockout mice did not proliferate in response to LPS or lipid A stimulation *ex vivo* [6]. A similar result was also found using B cells from Myd88 knockout mice, an adaptor protein that links TLRs to downstream signalling [15].

An important component of both TD and TI responses is B cell proliferation. It is likely that changes in metabolic requirements and energy demand to support proliferation will require changes in the proteome of the B cells. [16]. Naïve B cells have been shown to remain in a quiescent state with low metabolic demand [17]. However, upon activation using LPS or anti-IgM to stimulate the BCR, both glucose uptake and oxygen consumption rate are increased [18 19].

In the present study, we use Data Independent Acquisition (DIA) based mass spectrometry to map proteomic changes in B cells following activation with LPS and Interleukin 4 (IL-4) *ex vivo*. This revealed important roles for amino acid uptake and cholesterol metabolism in the proliferative response to LPS stimulation.

Results

LPS + IL-4 stimulation of naïve B cells promotes proliferation and changes the expression of enzymes involved in cell metabolism.

Previous studies have shown that *ex vivo* stimulation of murine B cells with LPS and IL-4 can drive B cell proliferation and class switching to IgG1 [20]. Consistent with this we found that stimulation of lymphocytes isolated from lymph nodes and subsequently stimulated with LPS + IL-4 resulted in the proliferation of CD19+ B cells, as judged by dilution of Cell Trace Violet (CTV) labelling. LPS + IL-4 stimulation leads to extensive proliferation with up to 6 generations of B cells present after 72 hours (Figure 1A). Proliferation itself is thought to be a prerequisite for cells to undergo class-switching [21]. In line with this, only LPS + IL-4 stimulated B cells found in later generations were positive for IgG1 (Figure 1A). On a similar note, cell size is considered a key regulator of the G1/S transition, as progression through the cell cycle can only continue once a certain threshold in size has been reached [22]. Accordingly, we found that 72 hours of LPS + IL-4 stimulation led to a marked increase in cell size and granularity as indicated by a higher forward/side scatter (Figure 1B-D). Stimulation with IL-4 alone resulted in a smaller increase in cell size than a combination of LPS and IL-4 but did not give rise to a strong proliferative response or class switching (Figure 1A-D).

These functional changes seen following activation suggest a significant change in regulation is occurring at the protein level. To investigate this further, we performed DIA-based mass spectrometry to compare the proteome of B cells after 24 hours of LPS + IL-4 stimulation to that of naive B cells. Using this approach a total of 8030 protein species were identified, of which 7187 were quantified in both naïve and LPS + IL-4 stimulated cells. Based on the mass spectrometry data, the predicted total protein mass in the B cells increased by approximately 2-fold following stimulation with a combination of LPS + IL-4 (Figure 1E). The proteomic ruler method [23], was used to estimate protein copy numbers and concentration then used to calculate fold changes between naïve and LPS + IL-4 stimulated B cells. This change in mass was due to an increased copy number of most proteins in the cell (Figure 1F), with a median $\log_2$ fold increase of 1.04. To adjust for the increase in cell size, the fold change in protein concentration was used as this could provide an indication of which proteins may be enriched, up or down, following LPS + IL-4 treatment, over those changing proportionally with cell size.

Using cutoffs of $q < 0.05$ and a $\log_2$ fold change more than one standard deviation away from the median, 863 proteins were found to be enriched following activation while a further 301 were detected in all the stimulated B cells but none of the naïve ones. 409 proteins were downregulated in the LPS + IL-4 stimulated cells in comparison to naïve B cells, while a further 57 were detected in the naïve B cells but none of the activated B cells (Figure 1G).

To identify the biological pathways which were affected by LPS + IL-4 stimulation, the enriched proteins were searched against the Gene Ontology (GO) Biological Processes, Uniprot Keyword Biological Process and *Kyoto Encyclopaedia of Genes and Genomes* (KEGG) databases. Enrichment analysis on the downregulated proteins did not highlight any specific processes. However, upregulated proteins were associated with terms related to the cell cycle, ribosome biogenesis, protein translation and steroid biosynthesis (Figure 1H, Table S1).

While these processes would make sense in terms of cell proliferation, it was notable that changes in the glycolytic and oxidative phosphorylation pathways were not highlighted in this analysis. Previous studies have indicated that there is an increased demand for glucose in LPS activated B cells [18,24]. Isotope tracing experiments following CD40L and IL-4 activation to stimulate proliferation have suggested that this increased glucose uptake is used in the pentose phosphate pathway, potentially to provide NADPH and precursors for nucleotide biosynthesis while alternative carbon sources are used to drive an increase in the TCA cycle and oxidative phosphorylation [17]. The levels of enzymes involved in glucose metabolism was examined in the proteomic data.

B cells express the SLC2A1 (Glut1) glucose transporter and deletion of this gene has been shown to reduce B cell activation *in vivo* [25,26]. There was a small increase in the concentration of SLC2A1, which would be consistent with an elevated ability to take up glucose (Figure S1E). In addition, there was a 25-fold increase in hexokinase 2 (HK2), one of the enzymes involved in catalysing the 1st committed step for glucose to enter the glycolytic or pentose phosphate pathways [27] (Figure S1F) and which has recently been shown to be required for maximal B cells responses to *ex vivo* stimulation with LPS [28]. In general, large changes in the estimated concentrations of proteins involved in glycolysis, pentose phosphate pathway, TCA cycle or oxidative phosphorylation were not observed (Figure S1A, B), although their copy numbers did increase in proportion to the increase in cell size (Figure S1C, D). To investigate if the increased copy number of ETC proteins correlated with changes in mitochondrial mass, B cells were stained with MitoTracker, a fluorescent dye that binds to mitochondria. We found that mitochondrial mass was significantly increased following 24 hours of LPS + IL-4 stimulation (Figure S1G, H).

B cell activation upregulates proteins involved in the cell cycle

Stimulation with LPS + IL-4 causes B cells to exit from a quiescent state and start to proliferate (Figure 1). This was confirmed using DAPI staining, which demonstrated that while naïve B cells were predominantly in a G0/1 state, after 24 hours of LPS + IL-4 stimulation the proportion of B cells in the S and G2 stages of the cell cycle was increased (Figure 2A, B). Progression through G1 is associated with an increase in Cyclin D expression, and activation of CDK4 and 6 [29]. At the same time inhibitory cell

cycle proteins such as p27Kip1 (Cdkn1b) are downregulated [30]. We therefore analysed the proteomic data for evidence of these changes. In naïve B cells, Cyclin D was not detected while levels of CDK4 and 6 were low. The levels of Cyclin D, CDK4 and CDK6 were all increased following stimulation (Figure 2C-E). Naïve B cells expressed high levels of p27Kip1, and this was reduced by LPS + IL-4 stimulation (Figure 2F).

Unphosphorylated RB1 binds to the E2F1/2/3 transcription factor, preventing the transcription of genes required for cell cycle progression. Increased CDK4/6 activity initiates RB1 phosphorylation, reducing its interaction with E2F, and resulting in the induction of E2F target genes, allowing progression through G1 to the S phase of the cell cycle [29,31]. Increased phosphorylation of RB1 was observed in B cells following LPS+ IL-4 stimulation (Figure 2G, H). In line with the increased RB1 phosphorylation, the levels of protein expressed from known E2F target genes, such as *Mcm2-7, Pcna, Dhfr, Rrm1/2* and *Pola* [31,32,33], were increased following LPS + IL-4 stimulation (Figure 2I). Further progression through the cell cycle requires Cyclins E, A and B as well as CDK2 and CDK1. While Cyclin E was not detected in the proteomic data, the levels of Cyclin A, Cyclin B, CDK2 and CDK1 were all increased by LPS + IL-4 stimulation (Fig 2J-M).

Protein synthesis in LPS + IL-4 stimulated B cells is dependent on the uptake of amino acids

The cell growth and proliferation promoted by LPS + IL-4 stimulation would be expected to require an increased rate of protein synthesis. This is consistent with the proteomic analysis, which demonstrated an increase in total protein content within activated B cells (Figure 1E) and an enrichment of proteins associated with protein translation including proteins that regulate ribosome biogenesis and the ribosomes themselves (Figure 1H). The ribosome is composed of the 40S and 60S subunits, each of which is composed of multiple protein subunits [34]. LPS + IL-4 stimulation increased the total concentration of ribosomal proteins that make up both the 40S and 60S subunits (Figure 3A, B). This overall increase was due to higher expression of most of the individual proteins that make up the subunits, rather than a large increase in one or two of the proteins (Figure 3E, F). In line with the increase in ribosomal proteins, there was also an upregulation of proteins associated with ribosome biogenesis (Figure 3C, D, G). To determine if this correlated with an increased rate of protein synthesis, we measured the incorporation of the puromycin analog o-propargyl-puromycin (OPP) into newly synthesised proteins. Consistent with the upregulation of ribosomal proteins and biogenesis, OPP incorporation was significantly higher in B cells stimulated with LPS + IL-4 for 24 hours compared to naive B cells (Figure 3H-I).

Elevated protein synthesis during rapid proliferation would require an increased [23] supply of amino acids, which could not be completely satisfied by internal sources of

amino acids within the B cell. Several amino acid transporters were detected in the proteomic analysis, and these were all found to be upregulated in response to stimulation with LPS + IL-4 (Figure 4A). To look at the requirement for increased amino acid uptake for B cell proliferation more closely we focused on the Lat1 transporter, a member of the System L transporters. Lat1 is a heterodimer composed of an amino acid transporting light chain subunit, SLC7A5, and a chaperone heavy chain subunit, SLC3A2 (CD98) [35]. SLC3A2 can also dimerise with some other amino acid transporters. Both of these subunits were upregulated in the proteomic data following LPS + IL-4 treatment (Figure 4B, C), and the upregulation of SLC3A2 was confirmed by flow cytometry (Figure 4D, E).

Slc7a5$^{fl/fl}$/Vav-iCre$^{+/-}$ mice, which have a deletion of SLC7A5 in all hematopoietic cells, have a comparable number of naive B cells to wild-type (WT), littermate controls, indicating that SLC7A5 is not critical for initial B cell development [36]. To examine how the loss of SLC7A5 affects B cell proliferation in response to LPS + IL-4 stimulation, B cells were isolated from wild-type (WT) and *Slc7a5*$^{fl/fl}$/Vav-iCre$^{+/-}$ mice, labelled with CTV, and stimulated for 72 hours *ex vivo* with LPS + IL-4. While WT B cells proliferated, the majority of the *Slc7a5*$^{fl/fl}$/Vav-iCre$^{+/-}$ B cells failed to divide, and the number of viable B cells after 72 hours was much lower compared to WT B cells (Figure 4F, G). In line with the failure to proliferate, there was no evidence of class switching in the remaining *Slc7a5*$^{fl/fl}$/Vav-iCre$^{+/-}$ cells (Figure 4H, I). SLC7A5 transports large neutral amino acids, including phenylalanine, histidine, methionine, tryptophan and isoleucine, as well as the tryptophan metabolite kynurenine [37]. As kynurenine is fluorescent and its uptake can be measured by flow cytometry, the effect of LPS + IL-4 treatment on kynurenine uptake in B cells was determined. In line with the increased expression of SLC7A5 in LPS + IL-4 treated B cells; kynurenine uptake was also higher in B cells treated with LPS + IL-4 for 24 hours compared to naive B cells (Figure 4J). Kynurenine uptake in the LPS+IL-4 stimulated B cells was reduced by the competitive substrate 2-aminobicyclo-(2,2,1)-heptane-2-carboxylic acid (BCH), which inhibits uptake through System L transporters. Kynurenine uptake in *Slc7a5*$^{fl/fl}$/Vav-iCre$^{+/-}$ B cells was similar to the uptake in BCH-treated WT cells suggesting that SLC7A5 was the major system L transporter in LPS + IL-4 stimulated B cells (Figure 4J). BCH or SLC7A5 knockout did not reduce kynurenine uptake to baseline levels indicating that other transport mechanisms for kynurenine uptake exists in B cells. Incubation of the LPS + IL-4 stimulated B without kynurenine was used as an uptake control (Figure 4J). Similar results were obtained for B cells stimulated with LPS in the absence of IL-4 (Figure S2A).

Cholesterol metabolism is upregulated in activated B cells

The enrichment analysis (Figure 1H) suggested that sterol biosynthesis may be upregulated by LPS + IL-4 stimulation. Sterol biosynthesis allows the generation of cholesterol from Acetyl CoA within the cell via a complex multistep process (Figure

S3A). The 1st half of this pathway, often referred to as the mevalonate pathway, results in the production of farnesyl pyrophosphate [38]. This can then be used for several purposes in the cell including the synthesis of cholesterol via the Bloch or Kandutsch-Russell pathways [39], prompting us to investigate this pathway further. Analysis of proteomic data showed that the majority of enzymes involved in cholesterol biosynthesis were increased in LPS + IL-4 stimulated cells relative to naive B cells (Figure 5A). Cholesterol biosynthesis is controlled by 2 rate-limiting steps, the conversion of HMG-CoA to mevalonic acid which is catalysed by HMG-CoA-reductase (HMGCR) and the conversion of squalene to 2,3(*S*)-oxidosqualene catalysed by squalene monooxygenase (SQLE) [38]; while neither of these enzymes were detected in the proteomic dataset for the naive B cells they were both robustly expressed in the LPS + IL-4 stimulated samples (Figure 5B, C). Cells can also obtain cholesterol via the uptake of low-density lipoprotein (LDL) through the low-density lipoprotein receptor (LDLR) [40]. Similar to HMGCR and SQLE, the LDLR was not found in naive B cells but was detected in B cells following LPS + IL-4 stimulation (Figure 5D). Together the above results suggest that LPS + IL-4 treatment would drive an increase in cellular cholesterol.

To test this, B cells were stained with the fluorescent dye filipin which binds to cellular cholesterol. LPS + IL-4 stimulation resulted in a gradual increase in cholesterol levels from 8 hours to 24 hours of stimulation (Figure 5E). As cells can obtain cholesterol via *de novo* synthesis or uptake of LDL from serum, we compared the effects of culturing B cells in normal serum or serum treated with fumed silica to remove LDL [41]. Analysis of the serum indicated that this treatment successfully removed LDL and HDL but did not affect the levels of triglycerides (Table S2). Since culturing B cells in cholesterol free media resulted in a higher level of filipin staining (Figure 5I) we titrated inhibitors of cholesterol biosynthesis in this, to see what concentration was required to reduce filipin staining.

This increase in cholesterol could be blocked by the HMGCR inhibitors Fluvastatin or Rosuvastatin or by NB-598, an inhibitor of SQLE (Figure 5F-H). Cells remained viable after 24 hours of inhibitor treatment (Figure S4). Furthermore, the ability of HMGCR inhibition to reduce cholesterol levels did not correlate with effects on cell size, as judged by FSC measurements by flow cytometry after 24 hours (Figure S4). Unexpectedly LPS + IL-4 treatment resulted in a higher level of cholesterol in the cells cultured in cholesterol-free media compared to normal media (Figure 5I). Similar to normal media, the increase in filipin staining in the cells grown in cholesterol-free media was blocked by treatment with either Fluvastatin or NB-598 (Figure 5I).

Cholesterol biosynthesis is critical for the survival and proliferation of LPS + IL-4 stimulated B cells

As the above data indicated that B cells upregulate cholesterol biosynthesis following LPS + IL-4 stimulation, we assessed the importance of this process for B cell

proliferation *ex vivo.* Stimulation with LPS + IL-4 for 48 hours in normal media promoted B cell proliferation, as shown by an increase in cell number and CTV staining (Figure 6A, B). This was accompanied by an increase in cell size, as judged by an increase in forward scatter (FSC) (Figure 6C). Treatment with either Fluvastatin or NB-598 resulted in a greatly decreased number of live cells and cell size at 48 hours of LPS + IL-4 stimulation, with no evidence of cell division after CTV staining (Figure 6A-C). Stimulation of B cells with LPS + IL-4 in cholesterol-free media resulted in more live B cells than stimulation in normal media, and the cells had on average undergone more divisions than B cells cultured in normal media (Figure 6A-C). Similar to their effects in normal media, Fluvastatin and NB-598 reduced B cell proliferation and survival in response to LPS + IL-4 stimulation in cholesterol-free media (Figure 6A-C).

To test the dependence of cholesterol uptake by the LDLR on B cell proliferation we isolated B cells from WT and *Ldlr-/-* mice before labelling with CTV and stimulating with LPS + IL-4 for 48 hours. Stimulation of WT B cells promoted proliferation, as judged by an increase in cell number, forward scatter and percentage of B cells in later generations based on CTV staining. (Figure 6D-F). Conversely, the number of live B cells and forward scatter of *Ldlr-/-* mice was reduced following LPS + IL-4 stimulation (Figure 6D,E). Similarly, the proportion of proliferating B cells was lower in *Ldlr-/-* compared to WT mice, suggesting that B cells from *Ldlr-/-* was slower.

In addition to cholesterol biosynthesis, the mevalonate pathway is also required for protein prenylation (Figure S3A). As SQLE acts downstream of this branch point, the effects of NB-598 would argue for an important role of cholesterol in LPS + IL-4 induced proliferation, however they would not exclude a parallel role for protein prenylation in this process. Prenylation typically involves the addition of a farnesyl or geranylgeranyl motif to cysteine residues near the C-terminus of target proteins and has been linked to proliferation in several cell types [42,43]. To determine if the inhibitory effects of Fluvastatin may be in part due to changes in prenylation, B cells were treated with a prenylation inhibitor (FGTI-2734) [44] prior to stimulation with LPS + IL-4 for 48 hours. The increase in B cell number seen following LPS + IL-4 stimulation was completely abolished in both normal and cholesterol-free media following FGTI-2734 treatment (Figure 6G) and in line with this, CTV labelling showed no evidence for cell division in the surviving FGTI-2734 treated cells (Figure 6H). FGTI-2734 also blocked the increase in cell size in response to LPS + IL-4 treatment (Figure 6I).

Cholesterol is required for B cell proliferation in response to multiple agonists

While the above results indicate that cholesterol is required for B cell proliferation in response to LPS + IL-4 stimulation, they do not demonstrate if the primary signal for this is LPS or IL-4. To test this, B cells were stimulated with either IL-4, LPS or a combination of both and changes in cholesterol were measured by filipin staining.

Stimulation with either LPS or IL-4 for 24 hours was able to increase B cell cholesterol levels, although LPS had a greater effect (Figure 7A).

Given the effects of HMGCR inhibition, and subsequent reduction in cholesterol levels as determined by filipin staining on LPS-induced B cell proliferation in the absence of IL-4 (Figure 7A), we also tested if other stimuli known to activate B cells could also increase cholesterol levels. Mouse B cells also respond to TLR7 [45] and TLR9 [46,47] agonists as well as the TLR4 agonist LPS [6]. Both the TLR7 agonist Resiquimod and the TLR9 agonist CpG increased cholesterol levels in B cells (Figure 7B). Naive B cells can also be activated by ligation of their BCR with anti-IgM antibodies, or by stimulation with CD40 ligand (CD40L). Similar to TLR agonists, both of these stimuli also increased cholesterol levels in B cells (Figure 7B). Resiquimod, CpG, anti-IgM and CD40L were all able to stimulate proliferation, as evidenced by CTV labelling after 72 hours of treatment (Figure 7C, D). While none of these stimuli were as effective at inducing proliferation as LPS, in each case, treatment with Fluvastatin blocked the proliferation (not shown) and survival of the B cells (Figure 7C).

Discussion

Upon stimulation, naive B cells can exit their quiescent state and start to proliferate. LPS is a well-established mitogen for murine B cells[6,48], therefore we used proteomics to investigate the changes that LPS stimulates in B cells to induce proliferation. In response to LPS + IL-4 stimulation *ex vivo*, B cells were able to rapidly expand and proliferate, eventually undergoing CSR to produce IgG1 (Figure 1). In this system, LPS is the main driver of proliferation, as B cells stimulated with LPS alone (Figure 7C) were able to proliferate but cells stimulated with IL-4 alone did not (Figure 1A). IL-4 may assist B cell survival and can promote CSR to the IgG1 isoform[20,49].

Analysis of the naive and 24 hour LPS + IL-4 activated B cell proteomes showed increased levels of Cyclin D, CDK4 and CDK6, which promote entry and progression through G1 and reduced levels of the cell cycle inhibitor p27Kip1 (Figure 2). While these changes are not unexpected, it illustrates the potential of the proteomic dataset to highlight processes important for B cell proliferation. GO term Enrichment analysis indicated that proteins involved in protein synthesis, amino acid uptake and cholesterol metabolism were highly upregulated, thus these processes were investigated further.

One of the most apparent effects of LPS + IL-4 stimulation was to increase the protein mass of the individual B cells, which was accompanied by an increase in ribosomal proteins and the rate of protein synthesis (Figure 3). In order to synthesise new proteins, get bigger and divide, B cells would require more amino acids than they would be able to generate by protein recycling. For essential amino acids, this would require the import of amino acids from the environment. Upon activation, B cells upregulated several amino acid transporters including the system L transporters SLC7A5 and 6 (Figure 4A), which can import large neutral amino acids, including the essential amino acids histidine, isoleucine, leucine, methionine, phenylalanine,

threonine, tryptophan and valine [37]. Of these, SLC7A5 was expressed at a higher level and was responsible for the majority of amino acid uptake via system 1 transporters. Amino acid uptake was sensitive to the competitive substrate BCH (Figure 4J), which blocks both SLC7A5 and 6. The cationic amino acid transporter SLC7A1, which can import the conditionally essential amino acids lysine and arginine, was also upregulated (Figure 4A).

Knockout of SLC7A5 in either hematopoietic cells or B cells has been previously shown not to affect the number of splenic B cells in mice[36], although a decrease in the number of peritoneal B1 cells was reported[50]. Although not critical for initial B cell development, SLC7A5 was critical for the expansion of B cells in response to *ex vivo* stimulation with LPS (Figure 4). This suggests that the B cells may rely on different amino acid transporters at different points in their development. A similar observation has been made in T cells, where SLC7A5 in not required for T cell development but is required for the clonal expansion and effector functions of T cells following activation via the T cell receptor[36].

In addition to increased uptake, B cells have also been reported to increase amino acid biosynthesis under certain conditions. ssRNAseq has shown that cycling B cells express higher levels of mRNA for enzymes in the serine biosynthetic pathway[53]. Furthermore, these proteins, as well as serine biosynthesis, were found to be increased by stimuli, such as anti-IgM, CD40L and CpG, that are known to induce B cell proliferation[53]. While not directly addressed in the current study, the proteomic data reported here also demonstrates the upregulation of serine biosynthetic enzymes, including the rate limiting enzyme PHDGH, in response to LPS + IL-4 stimulation (Figure S5).

Proliferating cells also need to generate new membranes as they increase in size, before undergoing cell division. Consistent with this, lipidomic studies have reported that LPS activated B cells have a higher total lipid content than naive B cells[54]. In addition to phospholipids and sphingolipids, cell membranes also contain cholesterol. Interestingly while LPS + IL-4 upregulated proteins were not enriched for proteins involved in phospholipid and sphingolipid biosynthesis, there was a strong enrichment for proteins involved in cholesterol biosynthesis (Figure 1, H). In line with this, there was also an increase in the cholesterol content of B cells following stimulation (Figure 5). Recently IL-4 has been described to upregulate the cholesterol biosynthetic pathway and prime cells for proliferation in response to CD40 stimulation[55]. Consistent with this report we also found that IL-4 alone could upregulate cholesterol levels, however this was not as great as LPS alone (Figure 7A). We also noted that several other B cell activating stimuli, including CD40L, could increase cholesterol levels (Figure 7A).

Cholesterol homeostasis is regulated by the SREBP2 transcription factor, which is found as an immature precursor protein embedded in the endoplasmic reticulum (ER) with chaperones SCAP and INSIG[40,56]. Low sterol levels are detected by the sterol sensing domain of SCAP, leading to the dissociation and degradation of INSIG.

Subsequently, the SCAP-SREBP2 complex is transported from the ER to the Golgi apparatus where it interacts with site 1 and site 2 proteases, allowing cleavage of SREBP2. The mature form of SREBP2 translocates to the nucleus, resulting in the upregulation of genes involved in cholesterol metabolism, including HMGCR, SQLE and LDLR. The importance of SREBP regulation *in vivo* for B cell function has recently been demonstrated using B cell specific knockouts of SCAP. In these mice, geminal centre formation and antibody responses to immunisation were compromised. Furthermore, B cells from these mice did not respond to mitogenic stimulation in part due to an inability to increase cellular cholesterol[57].

B cells can obtain cholesterol either via biosynthesis or uptake, the main route for which would be the uptake of LDL via the LDLR. In media lacking LDL, LPS could still stimulate an increase in cellular cholesterol (Figure 5I) and drive proliferation, and this could be blocked by inhibition of HMGCR or SQLE (Figure 6). Interestingly, B cells proliferated faster in cholesterol free media in response to LPS + IL-4 stimulation, whereas deletion of the LDLR resulted in B cells that proliferated more slowly than WT cells (Figure 6D, E). Previous work in CD8 T cells has shown that signalling pathways downstream of mTORC1 were differentially regulated between *Ldlr-/-* CD8 T cells and WT CD8 T cells. Additionally, the delivery of cholesterol to the lysosome by lipoproteins via the LDLR triggered mORC1 activation resulting in CD8 T cell activation, proliferation and metabolic reprogramming [58]. Thus, while the LDLR may regulate upstream from mTORC1 signalling, blocking HMGCR may be inhibiting processes downstream of mTORC1.

Farnesyl-pyrophosphate is an intermediate in cholesterol biosynthesis that it is also required for protein prenylation. As a result, HMGCR inhibitors will block prenylation in addition to protein synthesis. Canonical prenylation pathways typically involves the addition of farnesyl or geranylgeranyl lipids onto the cysteine residue in a CAAX motif in target proteins via the enzymes protein farnesyltransferase (FTase) or protein geranlygeranyltransferase I (GGTase I)[59]. We found that FGTI-2734, an inhibitor of FTase and GGTase, blocked LPS induced B cell proliferation (Figure 6G-I), suggesting an important role for prenylation in B cells. As inhibition of SQLE, which is downstream of farnesyl-pyrophosphate in cholesterol biosynthesis also blocked B cell proliferation it is likely that HMGCR inhibition will have a dual effect on B cell activation via both cholesterol synthesis and prenylation. Of note, the inhibition of HMGCR with Atorvastatin has been shown to inhibit the proliferation of B cells isolated from human blood following CD40L stimulation[60]. In this study, the addition of geranylgeranyl pyrophosphate rescued the effect of Atorvastatin on the upregulation of the activation markers CD80 and CD86, suggesting that in these cells prenylation, and not cholesterol biosynthesis is regulated by HMGCR. This study did not however look at the ability of geranylgeranyl pyrophosphate to rescue proliferation, or if the requirement for cholesterol could be satisfied by cholesterol uptake from the environment.

Overall, the proteomic analysis described here supports the concept that B cells undergo a major reorganization of metabolic pathways following TLR activation and that this is required to support a switch from quiescence to an activated state.

Resource availability

Lead contact

Further information and requests for resources should be directed to and will be fulfilled by the lead contact, Simon Arthur (j.s.c.arthur@dundee.ac.uk).

Materials availability

This study did not generate new unique reagents.

Data availability

The mass spectrometry proteomics data have been deposited to the ProteomeXchange Consortium (http://proteomecentral.proteomexchange.org) via the PRIDE partner repository [61] with the dataset identifier PXD057739. Flow cytometry data that support the findings of this study are available from the corresponding author upon request.

Any additional information required to reanalyse the data reported in this paper is available from the lead contact upon request.

Acknowledgments

The authors thank A. Rennie and R. Clarke from the Flow Cytometry Facility for cell sorting and advice on flow cytometry. We also thank the FingerPrints Proteomics facility for running our samples for mass spectrometry and for advice on proteomics. This research was supported by a Wellcome Trust PhD studentship award (DMSC, UNS148487).

Author contributions

D.M.S.C., M.R., S.A., performed the experiments. F.B. performed experiments using Ldlr-/- mice. A.J.M. performed the liquid chromatography–mass spectrometry.

D.M.S.C and J.S.C.A analysed the proteomics data. L.V.S designed the kynurenine uptake and protein synthesis experiments. M.S optimised the silica depletion and filipin staining experiments. D.M.S.C and J.S.C.A wrote the manuscript.

Declaration of interests

The authors declare no competing interests

Supplemental information

Table S1. Excel file containing terms for protein enrichment too large to fit in a pdf. Related to Figure 1H.

Table S2. Serum tests related to Figure 5.

Table S3. Statistics table related to all figures.

Methods

Mice

C45Bl6/J mice were obtained from Charles River Laboratories or bred in-house. Conditional *SLC7A5* knockout mice bred to Vav-iCre mice have been described previously and were maintained on a CBA/Ca×C57F7BL/10 background [36,62,63]. The mice were kept in individually ventilated cages, under specific pathogen-free conditions. Mice were given free access to food (RM3 irradiated pelleted diet, Special Diet Services) and water. Animal rooms were maintained at 21°C and a humidity of 45 to 55% with a 12/12 h light cycle. Mice were sacrificed using a rising concentration of CO2 and death was confirmed by either cervical dislocation or exsanguination. All animal work was approved by the University of Dundee's Welfare and Ethical Use of Animals Committee and in accordance with UK and EU law.

WT and *Ldlr −/−* male and female mice on C57BL/6J background were obtained from The Jackson Laboratory. The mice were kept in individually ventilated cages, under specific pathogen-free conditions. Mice were given free access to food and water. Animal rooms were maintained at 20 ± 2°C and a humidity of 50 ± 5% with a 12-h light/dark cycle. Mice were sacrificed using a rising concentration of CO2. All animal work conformed to the guidelines from 2010/63/EU directive of the European Parliament on the protection of animals used for scientific purposes and were approved by the Ethical Committee of the University of Milan and Italian Ministry of Health.

Cell isolation

Lymph nodes were homogenised through a 40μM cell strainer in DPBS buffer (Gibco) and after centrifugation at 450g for 4 minutes, the pellet was resuspended in DPBS. Lymphocytes were counted on a Novocyte (Agilent Technologies) and seeded at 1×10^6 cells/ml in B cell medium (RPMI-1640 supplemented with 10% FBS, 50 U/ml penicillin-streptomycin, 5mM L-glutamine, 10mM HEPES buffer, 1mM sodium pyruvate, 50 μM 2-mercaptoethanol and non-essential amino acids) for stimulation.

Spleens were dissociated through a 40μM filter in DPBS buffer (Gibco) and after centrifugation at 450g for 4 minutes, the pellet was resuspended in 1ml of Red Blood Cell Lysing Buffer (Hybri-Max™, Sigma) for 4 minutes at room temperature to lyse red blood cells. The reaction was quenched by the addition of DPBS and the cells were pelleted by centrifugation at 450g for 4 minutes. The pellet was resuspended in 10ml DPBS before counting the splenocytes on a Novocyte. Splenocytes were seeded at 1×10^6 cells/ml in B cell medium for stimulation or further purification of B cells.

B cell isolation

To obtain an enriched population of B cells, magnetic sorting was used to remove non-B cells. Briefly, splenocytes were incubated with Fc receptor-blocking antiCD16/CD32 antibody (BD Pharmingen) for 5 minutes on ice. The cells were incubated with a mixture of biotin-labelled anti-mouse antibodies (10μg/ml) (Table 1) for 20 minutes on ice. Unbound antibody was removed by washing with 10ml Magnetic Activated Cell Sorting (MACS) buffer (DPBS + 0.5% BSA + 2mM EDTA) followed by centrifugation. The cells were then resuspended in MACS buffer with streptavidin microbeads (1:10) (Miltenyi Biotech) and incubated at 4ºC for 15 minutes. Miltenyi LD columns were calibrated by passing through 3ml of MACS buffer. Cells were washed with 10ml MACS buffer and centrifuged at 450g for 4 minutes to remove excess beads. The cell pellet was then resuspended in MACS buffer and separated using magnetic-activated cell sorting columns according to the manufacturer's instructions (Miltenyi Biotec). Single-cell suspensions were collected and B cell numbers and purity (CD19+) were measured on a NovoCyte. Typical purity levels were 97% CD19+ve B cells. B cells were seeded at 2×10^5 cells/ml of B cell medium for stimulation for flow cytometry experiments or 2×10^6 cells/ml of B cell medium for stimulation for immunoblotting. When stated, isolated B cells were stained with 2.5μM CellTrace™ Violet (ThermoFisher) at 37ºC for 20 minutes, then quenched in 10ml B cell medium before seeding at the required density.

Stimulations and inhibitors

Cells were rested at 37ºC for 1 hour. When required, the cells were treated with the appropriate inhibitor at the concentrations indicated in the figure legend: NB-598 (MedChemExpress), Fluvastatin sodium (TOCRIS), Rosuvastatin calcium (TOCRIS),

FGTI-2734 (MedChemExpress). A combination of 20µg/ml LPS (L2654, Sigma) and 10ng/ml IL-4 (214-14, Peprotech) was used to stimulate the cells unless otherwise stated in the figure legend. For some experiments, cells were treated with LPS or IL-4 alone, or with 1µg/ml Resiquimod/R848 (tlrl-r848, Invivogen), 1µg/ml ODN 2006 (tlrl-2006, Invivogen), 10µg/ml Anti-Mouse IgM µ chain (115-006-075, Stratech) or 10µg/ml CD40 ligand (8230-CL-050/CF, R&D).

Removal of cholesterol from serum

Lipid depletion was carried out by adding 20g/L of fumed silica to FBS and mixing overnight at 4^0C [41]. The following day the FBS was centrifuged at 3264g for 2 hours at 20^0C. The supernatant then underwent a second round of centrifugation at 185477.8g for 1 hour at 20^0C. The resulting delipidated FBS was used in place of normal FBS when making B cell culture medium. Samples of normal and cholesterol-free FBS samples were sent to London Health Company, who carried out tests to measure changes in triglycerides, cholesterol, high-density lipoprotein (HDL) and low-density lipoprotein (LDL).

Cell survival, proliferation and class switching assays

Following stimulation, cells were washed in Fluorescence Activated Cell Sorting (FACS) buffer (1% BSA, DPBS) and then incubated with Fc receptor-blocking antiCD16/CD32 antibody (BD Pharmingen) in FACS buffer for 15 minutes at 4ºC before staining with the appropriate fluorochrome-conjugated antibodies (Table 2) in FACS buffer for 20 minutes at 4ºC. The samples were washed with FACS buffer prior to resuspension in 0.25 µg of 7AAD. Flow cytometry data was collected on a Novocyte and analysed using FlowJo V.10 software (BD Biosciences). A representative gating strategy is shown in Figure S6A for lymph node/splenocyte isolation, and Figure S7B for B cell isolation.

Cell cycle analysis and p-Rb staining

Cells were washed in FACS buffer and then fixed using 1:1 IC fixation buffer (catalogue number: 00-8222-49, eBiosciences) and FACS buffer, and incubated at 4ºC for 20 minutes. Following another wash in FACS buffer, cells were resuspended in 100µl of cold ethanol and stored at -20ºC for 30 minutes. The samples were washed with FACS buffer twice before incubation with Fc receptor-blocking anti-CD16/CD32 antibody (BD Pharmingen) in FACS buffer for 15 minutes at 4ºC. Surface stains (Table 2) were incubated for 1 hour at room temperature before washing with FACS buffer and re-suspension in 0.5 µg/ml of DAPI . Flow cytometry data was collected on a Novocyte and analysed using FlowJo V.10 software (BD Biosciences). A representative gating strategy is shown in Figure S6B.

O-propargyl-puromycin uptake assay

Uptake of the puromycin analogue O-propargyl-puromycin was used to estimate protein synthesis rates. Splenocytes were stimulated with 20µg/ml LPS and 10ng/ml IL-4. After 24 hours the cells were treated with 20µM of O-propargyl-puromycin for 30 minutes at 37ºC. 100 µL of 2% paraformaldehyde in T/B media was added to 100ul cells before incubation in complete darkness at room temperature for 30 minutes. The samples were pelleted by centrifugation at 450g for 4 minutes before resuspension in 100µl of DPBS. Following this, the samples were washed with FACS buffer and then resuspended in 100µl of 0.01% Saponin (Sigma) in DPBS, before incubation at room temperature for 20 minutes. The samples were pelleted by centrifugation at 450g for 4 minutes before resuspension in 30µl of Click mixture 1mM Copper sulphate (209198, Sigma), 10mM Sodium ascorbate (A7631. Sigma), 1mM BTTAA (906328, Sigma), 10mM Aminoguanidine (81530, Cayman Chemicals), DPBS (14190144, Gibco), 5µM Alexafluor 647 azide (A10277, Invitrogen) and incubation in complete darkness at room temperature for 1 hour. The samples were pelleted by centrifugation at 450g for 4 minutes before resuspension in 200µl of FACS buffer and incubation in complete darkness at room temperature for 30 minutes. Again, the samples were pelleted by centrifugation at 450g for 4 minutes before washing again in FACS buffer. The cells were incubated with Fc receptor-blocking anti-CD16/CD32 antibody (BD Pharmingen) in FACS buffer for 15 minutes at 4ºC. Surface stains (Table 1) were incubated for 1 hour at room temperature. The samples were washed with FACS buffer prior to resuspension in 300µl FACS buffer. Flow cytometry data was collected on a Novocyte and analysed using FlowJo V.10 software (BD Biosciences). A representative gating strategy is shown in Figure S6C.

Kynurenine uptake assay

Uptake of the tryptophan metabolite kynurenine was used to estimate the uptake rates via neutral amino acid transporters [64]. Isolated B cells were stimulated with 20µg/ml LPS and 10ng/ml IL-4. After 24 hours the cells were washed in FACS buffer and then incubated with Fc receptor-blocking antiCD16/CD32 antibody (BD Pharmingen) in FACS buffer for 15 minutes at 37ºC before staining with CD19 APC (Table 2) in FACS buffer for 20 minutes at 37ºC. The samples were washed with FACS buffer and then resuspended in 0.2ml HBSS. Either 0.1ml of HBSS or 0.1ml of 40mM BCH was then added to each sample. After this, 100µl of 800µM Kynurenine was added and the samples were incubated for 5 minutes at 37ºC. After the 5 minutes, the samples were fixed by adding 125µl of 4% paraformaldehyde made in DPBS for 18 minutes at 4ºC. The samples were then washed 2 times with FACS buffer and re-suspended in 400µl of FACS buffer. Flow cytometry data was collected on an LSR Fortessa (BD biosciences) and analysed using FlowJo V.10 software (BD Biosciences). A representative gating strategy is shown in Figure S6D.

Cholesterol staining assay

Changes in cellular cholesterol content were determined using the cholesterol binding agent filipin [65]. Splenocytes were stimulated with 20µg/ml LPS and 10ng/ml IL-4. After 24 hours the cells were washed twice in DPBS before staining for viability using eFluor 660 fixable viability dye (Table 2) for 30 minutes at 4ºC using 1 x DPBS. After two washes in FACS buffer, the cells were fixed using 1:1 IC fixation buffer (catalogue number: 00-8222-49, eBiosciences) and FACS buffer, before incubation at 4ºC for 20 minutes. Following another wash in FACS buffer, cells were incubated with Fc receptor-blocking anti-CD16/CD32 antibody (BD Pharmingen) in FACS buffer for 15 minutes at 4ºC. Surface stains (Table 2) were incubated for 20 minutes at 4ºC. The samples were washed with FACS buffer prior to resuspension in 270µl FACS buffer and 30µl of 1µg/µl filipin (Merck) before incubation in complete darkness at room temperature for 30 minutes. Flow cytometry data was collected on an LSR Fortessa (BD biosciences) and analysed using FlowJo V.10 software (BD Biosciences). A representative gating strategy is shown in Figure S7A.

Mitochondria staining assay

Splenocytes were stimulated with 20µg/ml LPS and 10ng/ml IL-4. After 24 hours the cells were washed twice in FACS buffer. 50µl of prewarmed (37°C) staining solution containing 100nM MitoTracker probe (Invitrogen) in FACS buffer was added into the cells before incubation at 37°C for 20 minutes. The samples were washed with FACS buffer before incubation with Fc receptor-blocking anti-CD16/CD32 antibody (BD Pharmingen) in FACS buffer for 15 minutes at 4ºC before staining with the appropriate fluorochrome-conjugated antibodies (Table 2) in FACS buffer for 20 minutes at 4ºC. The samples were washed with FACS buffer prior to resuspension in 0.25 µg of 7AAD. Flow cytometry data was collected on a Novocyte and analysed using FlowJo V.10 software (BD Biosciences). A representative gating strategy is shown in Figure S7C.

Proteomics

Proteomic samples were processed as described by (cite Howden B cell paper if on BioRxiv at this point). Wildtype C57BL/6 mice (Charles Rivers) aged between 8 and 12 weeks were used for all proteomic experiments. Lymph nodes were extracted from mice, mashed in RPMI media before filtering through a 70 mm cell strainer. Naïve B cells were isolated to high purity by fluorescence-activated cell sorting. Lymphocytes were incubated with Fc receptor-blocking antiCD16/CD32 antibody (BD Pharmingen) in FACS buffer for 15 minutes at 4ºC before staining with fluorochrome-conjugated antibodies (Table 2) in FACS buffer for 20 minutes at 4ºC. The samples were washed with FACS buffer prior to resuspension in 0.5 µg/ml of DAPI. CD19+,CD93-, DAPI- cells were sorted using a Sony SH800 cell sorter. Sorted cells were washed twice with HBSS and snap frozen in liquid nitrogen to be stored at -80 °C until processing for

mass spectrometry. For B cell activation, lymphocytes were suspended at a final density of 1.5 million cells/ml in medium (RPMI-1640 containing glutamine supplemented with 10% FBS, 50 U/ml penicillin-streptomycin, 50 μM 2-mercaptoethanol) and activated for 24 hours in the presence of 20μg/ml LPS and 10ng/ml IL-4. After 24 hours cells were incubated with Fc receptor-blocking antiCD16/CD32 antibody (BD Pharmingen) in FACS buffer for 15 minutes at 4ºC before staining with fluorochrome-conjugated antibodies (Table 2) in FACS buffer for 20 minutes at 4ºC. The samples were washed with FACS buffer prior to resuspension in 0.5 μg/ml of DAPI. CD19+ and DAPI- were sorted and collected as described above. Cells were then washed 3 times in PBS and cell pellets frozen at -80ºC.

Cell pellets were lysed and proteins were digested following the protocol described by [66]. In brief, 400 ml of lysis buffer (5% sodium dodecyl sulfate, 50 mM triethylammonium bicarbonate (pH 8.5) and 10 mM tris(2-carboxyethyl)phosphine-hydrochloride) was added to each sample and lysates shaken at room temperature at 1000 rpm for 5 minutes before being incubated at 95 °C at 500 rpm for 5 minutes. Samples were allowed to cool and were then sonicated using a BioRuptor (15 cycles: 30 sec on and 30 sec off) and alkylated with 20 mM iodoacetamide for 1 h at 22 °C in the dark. To determine protein concentration the EZQ protein quantitation kit (Thermo) was used and protein cleanup and digestion was performed using S-TRAP mini columns (Protifi). Proteins were digested with trypsin at 1:20 ratio (enzyme:protein) for 2 hours at 47°C. Digested peptides were eluted from S-TRAP columns using 50mM ammonium bicarbonate, followed by 0.2% aqueous formic acid and 50% aqueous acetonitrile containing 0.2% formic acid. Peptides were dried by speedvac before resuspending in 1% formic acid. Peptide quantity was measured using the CBQCA kit (Thermo).

LC-MS/MS analysis

Peptides were analysed by single shot Data Independent Aquisiation (DIA) mass spectrometry as previously described [67,68]. 1.5 μg of peptide from each sample was injected onto a nanoscale C18 reverse-phase chromatography system (UltiMate 3000 RSLC nano, Thermo Scientific) and electrosprayed into an Orbitrap Exploris 480 Mass Spectrometer (Thermo Fisher). The following buffers were used for liquid chromatography: buffer A (0.1% formic acid in Milli-Q water (v/v)) and buffer B (80% acetonitrile and 0.1% formic acid in Milli-Q water (v/v). Samples were loaded at 10 μl/min onto a trap column (100 μm × 2 cm, PepMap nanoViper C18 column, 5 μm, 100 Å, Thermo Scientific) equilibrated in 0.1% trifluoroacetic acid (TFA). The trap column was washed for 3 min at the same flow rate with 0.1% TFA then switched in-line with a Thermo Scientific, resolving C18 column (75 μm × 50 cm, PepMap RSLC C18 column, 2 μm, 100 Å). Peptides were eluted from the column at a constant flow rate of 300 nl/min with a linear gradient from 3% buffer B to 6% buffer B in 5 min, then from 6% buffer B to 35% buffer B in 115 min, and finally to 80% buffer B within 7 min. The column was then washed with 80% buffer B for 4 min and re-equilibrated in 3% buffer

B for 15 min. Two blanks were run between each sample to reduce carry-over. The column was kept at a constant temperature of 50°C.

The data was acquired using an easy spray source operated in positive mode with spray voltage at 2.445 kV, and the ion transfer tube temperature at 250°C. The MS was operated in DIA mode. A scan cycle comprised a full MS scan (m/z range from 350 to 1650), with RF lens at 40%, AGC target set to custom, normalised AGC target at 300%, maximum injection time mode set to custom, maximum injection time at 20 ms, microscan set to 1 and source fragmentation disabled. MS survey scan was followed by MS/MS DIA scan events using the following parameters: multiplex ions set to false, collision energy mode set to stepped, collision energy type set to normalized, HCD collision energies set to 25.5, 27 and 30%, orbitrap resolution 30,000, first mass 200, RF lens 40%, AGC target set to custom, normalized AGC target 3000%, microscan set to 1 and maximum injection time 55 ms. Data for both MS scan and MS/MS DIA scan events were acquired in profile mode.

Proteomic data analysis

For comparing naïve and LPS stimulated B cells, raw mass spec data files were searched using Spectronaut version 19 (Biognosys). Data was analysed by DirectDIA. Raw mass spec data files were searched against a mouse database (Swissprot Trembl November 2023) with the following parameters: directDIA, false discovery rate set to 1%, protein N-terminal acetylation and methionine oxidation were set as variable modifications and carbamidomethylation of cysteine residues was selected as a fixed modification.

The following Spectronaut settings were used (Baker et al., 2024): all identification settings were set to 0.01 (precursor q-value cut-off, precursor PEP cut-off, protein FDR strategy (accurate), protein q-value cut-off (experiment), protein q-value cut-off (run) and protein PEP cut-off). The following quantification settings were used: ‘Quant 2.0’, the MS-Level quantity was set to ‘MS2’, imputation was disabled, major group Top N and minor group Top N were set as ‘False’ and cross run normalisation was set as ‘False’.

Intensity vales from Spectronaut were further analysed in Perseus [69] and the histone ruler method [23] used to estimate copy number and concentrations of the identified proteins. Fold change was calculated relative to levels in naïve B cells and significance determined using unpaired Students t tests on $\log_{10}$ transformed data. The False Discovery Rate approach using the 2-stage step up method Benjamini, Krieger, and Yekutieli [70] with a Q value of 0.01. Enrichment against the Gene Ontology (GO) Biological Processes, Uniprot Keyword Biological Process and *Kyoto Encyclopaedia of Genes and Genomes* (KEGG) databases. Biological Process GO terms [71] and KEGG pathways [72] was carried out using the DAVID gene enrichment site [73].

Statistical analysis

Unless otherwise stated, graphs show mean values + SD with individual replicates shown by symbols. Unpaired two-tailed Student's *t* test, one-way ANOVA or two-way ANOVA with post-hoc testing were performed in Prism and the tests used indicated in the figure legends. Full results of the ANOVA calculations are given in Table S3.

Table 1: MACS antibodies				
Antibody	Clone	Concentration	Catalogue number	Supplier
Anti-CD11b	M1/70	10µg/ml	101204	BioLegend
Anti-CD11c	N418	10µg/ml	117304	BioLegend
Anti-CD3ε	145-2C11	10µg/ml	100304	BioLegend
Anti-TER119	TER-119	10µg/ml	116204	BioLegend

Table 2: Flow cytometry antibodies					
Antibody	Fluorophore	Clone	Dilution	Catalogue number	Supplier
Anti-CD19	APC	6D5	1:300	115512	Biolegend
Anti-CD19	PE	1D3	1:200	557399	BD Biosciences
Anti-CD19	FITC	1D3	1:200	152403	BioLegend
Anti-CD93	APC	AA4.1	1:200	136510	BioLegend
Anti-CD98	PE	RL388	1:200	128208	BioLegend
dsDNA	eFluor 660	-	1:1000	65-0864-14	eBioscience
Anti-IgG1	FITC	A85-1	1:100	553443	BD Biosciences
Anti-pRb	FITC	D20B12	1:300	4277S	Cell Signaling Technology

References

1. Pone, E. J., Xu, Z., White, C. A., Zan, H. & Casali, P. B cell Toll-like receptors and immunoglobulin class-switch DNA recombination. *Frontiers in bioscience (Landmark edition)* **17**, 2594 (2012).
2. Stavnezer, J. Antibody class switching. *Adv Immunol* **61**, 79–146 (1996).
3. Hoffman, W., Lakkis, F. G. & Chalasani, G. B Cells, Antibodies, and More. *Clinical Journal of the American Society of Nephrology* **11**, 137 (2016).
4. De Silva, N. S. & Klein, U. Dynamics of B cells in germinal centres. *Nat Rev Immunol* **15**, 137–148 (2015).
5. Foote, J. B., Mahmoud, T. I., Vale, A. M. & Kearney, J. F. Long-Term Maintenance of Polysaccharide-Specific Antibodies by IgM-Secreting Cells. *The Journal of Immunology* **188**, 57–67 (2012).
6. Hoshino, K. *et al.* Cutting Edge: Toll-Like Receptor 4 (TLR4)-Deficient Mice Are Hyporesponsive to Lipopolysaccharide: Evidence for TLR4 as the Lps Gene Product1. *The Journal of Immunology* **162**, 3749–3752 (1999).
7. Poltorak, A. *et al.* Defective LPS signaling in C3H/HeJ and C57BL/10ScCr mice: mutations in Tlr4 gene. *Science* **282**, 2085–2088 (1998).
8. Coutinho, A., Gronowicz, E., Bullock, W. W. & Möller, G. MECHANISM OF THYMUS-INDEPENDENT IMMUNOCYTE TRIGGERING. *The Journal of Experimental Medicine* **139**, 74–92 (1974).
9. Dziarski, R. Preferential induction of autoantibody secretion in polyclonal activation by peptidoglycan and lipopolysaccharide. I. In vitro studies. *The Journal of Immunology* **128**, 1018–1025 (1982).
10. JOHNSON, A. G., GAINES, S. & LANDY, M. Studies on the O antigen of Salmonella typhosa. V. Enhancement of antibody response to protein antigens by the purified lipopolysaccharide. *The Journal of experimental medicine* **103**, 225–246 (1956).
11. Caroff, M. & Karibian, D. Structure of bacterial lipopolysaccharides. *Carbohydrate Research* **338**, 2431–2447 (2003).
12. Arthur, J. S. C. & Ley, S. C. Mitogen-activated protein kinases in innate immunity. *Nat Rev Immunol* **13**, 679–692 (2013).
13. Kawai, T., Ikegawa, M., Ori, D. & Akira, S. Decoding Toll-like receptors: Recent insights and perspectives in innate immunity. *Immunity* **57**, 649–673 (2024).
14. Triantafilou, M. & Triantafilou, K. Lipopolysaccharide recognition: CD14, TLRs and the LPS-activation cluster. *Trends in Immunology* **23**, 301–304 (2002).
15. Kawai, T., Adachi, O., Ogawa, T., Takeda, K. & Akira, S. Unresponsiveness of MyD88-Deficient Mice to Endotoxin. *Immunity* **11**, 115–122 (1999).
16. Peeters, R. & Jellusova, J. Lipid metabolism in B cell biology. *Molecular Oncology* **n/a**, (2023).

17. Waters, L. R., Ahsan, F. M., Wolf, D. M., Shirihai, O. & Teitell, M. A. Initial B Cell Activation Induces Metabolic Reprogramming and Mitochondrial Remodeling. *iScience* **5**, 99–109 (2018).
18. Dufort, F. J. *et al.* Cutting Edge: IL-4-Mediated Protection of Primary B Lymphocytes from Apoptosis via Stat6-Dependent Regulation of Glycolytic Metabolism1. *The Journal of Immunology* **179**, 4953–4957 (2007).
19. Jellusova, J. *et al.* Gsk3 is a metabolic checkpoint regulator in B cells. *Nat Immunol* **18**, 303–312 (2017).
20. Snapper, C. M., Finkelman, F. D., Stefany, D., Conrad, D. H. & Paul, W. E. IL-4 induces co-expression of intrinsic membrane IgG1 and IgE by murine B cells stimulated with lipopolysaccharide. *The Journal of Immunology* **141**, 489–498 (1988).
21. Hodgkin, P. D., Lee, J. H. & Lyons, A. B. B cell differentiation and isotype switching is related to division cycle number. *Journal of Experimental Medicine* **184**, 277–281 (1996).
22. Barberis, M., Klipp, E., Vanoni, M. & Alberghina, L. Cell Size at S Phase Initiation: An Emergent Property of the G1/S Network. *PLOS Computational Biology* **3**, e64 (2007).
23. Wiśniewski, J. R., Hein, M. Y., Cox, J. & Mann, M. A “Proteomic Ruler” for Protein Copy Number and Concentration Estimation without Spike-in Standards *. *Molecular & Cellular Proteomics* **13**, 3497–3506 (2014).
24. Johnstone, J. C., Yazicioglu, Y. F. & Clarke, A. J. Fuelling B cells: dynamic regulation of B cell metabolism. *Current Opinion in Immunology* **91**, 102484 (2024).
25. Bierling, T. E. H. *et al.* GLUT1-mediated glucose import in B cells is critical for anaplerotic balance and humoral immunity. *Cell Reports* **43**, 113739 (2024).
26. Brookens, S. K. *et al.* Plasma Cell Differentiation, Antibody Quality, and Initial Germinal Center B Cell Population Depend on Glucose Influx Rate. *The Journal of Immunology* **212**, 43–56 (2023).
27. Tanner, L. B. *et al.* Four Key Steps Control Glycolytic Flux in Mammalian Cells. *Cell Syst* **7**, 49-62.e8 (2018).
28. Paradoski, B. T. *et al.* PI3K-dependent reprogramming of hexokinase isoforms controls glucose metabolism and functional responses of B lymphocytes. *iScience* **27**, (2024).
29. Rubin, S. M., Sage, J. & Skotheim, J. M. Integrating Old and New Paradigms of G1/S Control. *Mol Cell* **80**, 183–192 (2020).
30. Wagner, E. F., Hleb, M., Hanna, N. & Sharma, S. A pivotal role of cyclin D3 and cyclin-dependent kinase inhibitor p27 in the regulation of IL-2-, IL-4-, or IL-10-mediated human B cell proliferation. *J Immunol* **161**, 1123–1131 (1998).
31. Engeland, K. Cell cycle regulation: p53-p21-RB signaling. *Cell Death Differ* **29**, 946–960 (2022).
32. Chicas, A. *et al.* Dissecting the unique role of the retinoblastoma tumor suppressor during cellular senescence. *Cancer Cell* **17**, 376–387 (2010).

33. Leone, G. *et al.* E2F3 activity is regulated during the cell cycle and is required for the induction of S phase. *Genes Dev* **12**, 2120–2130 (1998).
34. Doudna, J. A. & Rath, V. L. Structure and Function of the Eukaryotic Ribosome: The Next Frontier. *Cell* **109**, 153–156 (2002).
35. Napolitano, L. *et al.* LAT1 is the transport competent unit of the LAT1/CD98 heterodimeric amino acid transporter. *Int J Biochem Cell Biol* **67**, 25–33 (2015).
36. Sinclair, L. V. *et al.* Control of amino-acid transport by antigen receptors coordinates the metabolic reprogramming essential for T cell differentiation. *Nat Immunol* **14**, 500–508 (2013).
37. Fotiadis, D., Kanai, Y. & Palacín, M. The SLC3 and SLC7 families of amino acid transporters. *Molecular Aspects of Medicine* **34**, 139–158 (2013).
38. Buhaescu, I. & Izzedine, H. Mevalonate pathway: A review of clinical and therapeutical implications. *Clinical Biochemistry* **40**, 575–584 (2007).
39. Mitsche, M. A., McDonald, J. G., Hobbs, H. H. & Cohen, J. C. Flux analysis of cholesterol biosynthesis in vivo reveals multiple tissue and cell-type specific pathways. *eLife* **4**, e07999 (2015).
40. Luo, J., Yang, H. & Song, B.-L. Mechanisms and regulation of cholesterol homeostasis. *Nat Rev Mol Cell Biol* **21**, 225–245 (2020).
41. Brovkovych, V., Aldrich, A., Li, N., Atilla-Gokcumen, G. E. & Frasor, J. Removal of Serum Lipids and Lipid-Derived Metabolites to Investigate Breast Cancer Cell Biology. *PROTEOMICS* **19**, 1800370 (2019).
42. Blank, N. *et al.* Atorvastatin Inhibits T Cell Activation through 3-Hydroxy-3-Methylglutaryl Coenzyme A Reductase without Decreasing Cholesterol Synthesis1. *The Journal of Immunology* **179**, 3613–3621 (2007).
43. Su, W. *et al.* Protein Prenylation Drives Discrete Signaling Programs for the Differentiation and Maintenance of Effector Treg Cells. *Cell Metabolism* **32**, 996-1011.e7 (2020).
44. Kazi, A. *et al.* Dual Farnesyl and Geranylgeranyl Transferase Inhibitor Thwarts Mutant KRAS-Driven Patient-Derived Pancreatic Tumors. *Clinical Cancer Research* **25**, 5984–5996 (2019).
45. Weeratna, R. D., Makinen, S. R., McCluskie, M. J. & Davis, H. L. TLR agonists as vaccine adjuvants: comparison of CpG ODN and Resiquimod (R-848). *Vaccine* **23**, 5263–5270 (2005).
46. Arunkumar, N., Liu, C., Hang, H. & Song, W. Toll-like receptor agonists induce apoptosis in mouse B-cell lymphoma cells by altering NF-κB activation. *Cell Mol Immunol* **10**, 360–372 (2013).
47. Yi, A.-K., Chang, M., Peckham, D. W., Krieg, A. M. & Ashman, R. F. CpG Oligodeoxyribonucleotides Rescue Mature Spleen B Cells from Spontaneous Apoptosis and Promote Cell Cycle Entry1. *The Journal of Immunology* **160**, 5898–5906 (1998).
48. Poltorak, A. *et al.* Defective LPS Signaling in C3H/HeJ and C57BL/10ScCr Mice: Mutations in Tlr4 Gene. *Science* **282**, 2085–2088 (1998).
49. Moon, H. B. *et al.* Regulation of IgG1 and IgE synthesis by interleukin 4 in mouse B cells. *Scand J Immunol* **30**, 355–361 (1989).

50. Sun, Y., Wen, J., Xu, T. & Meng, L. Reduction of peritoneal cavity B1a cells in adult Slc7a5 knockdown mice via dysregulating the mTOR pathway. *Int Immunopharmacol* **117**, 109939 (2023).
51. Goul, C., Peruzzo, R. & Zoncu, R. The molecular basis of nutrient sensing and signalling by mTORC1 in metabolism regulation and disease. *Nat Rev Mol Cell Biol* **24**, 857–875 (2023).
52. Howden, A. J. M. *et al.* Quantitative analysis of T cell proteomes and environmental sensors during T cell differentiation. *Nat Immunol* **20**, 1542–1554 (2019).
53. D'Avola, A. *et al.* PHGDH is required for germinal center formation and is a therapeutic target in MYC-driven lymphoma. *J Clin Invest* **132**, e153436 (2022).
54. Ma, C. *et al.* Upregulated selenoprotein I during lipopolysaccharide-induced B cell activation promotes lipidomic changes and is required for effective differentiation into IgM-secreting plasma B cells. *Journal of Leukocyte Biology* **116**, 6–17 (2024).
55. Steach, H. R. *et al.* IL-4 Licenses B Cell Activation Through Cholesterol Synthesis. 2024.05.13.593964 Preprint at https://doi.org/10.1101/2024.05.13.593964 (2024).
56. Brown, M. S., Radhakrishnan, A. & Goldstein, J. L. Retrospective on Cholesterol Homeostasis: The Central Role of Scap. *Annu Rev Biochem* **87**, 783–807 (2018).
57. Luo, W. *et al.* SREBP signaling is essential for effective B cell responses. *Nat Immunol* **24**, 337–348 (2023).
58. Bonacina, F. *et al.* The low-density lipoprotein receptor–mTORC1 axis coordinates CD8+ T cell activation. *The Journal of Cell Biology* **221**, e202202011 (2022).
59. Wang, M. & Casey, P. J. Protein prenylation: unique fats make their mark on biology. *Nat Rev Mol Cell Biol* **17**, 110–122 (2016).
60. Shimabukuro-Vornhagen, A. *et al.* Inhibition of Protein Geranylgeranylation Specifically Interferes with CD40-Dependent B Cell Activation, Resulting in a Reduced Capacity To Induce T Cell Immunity. *The Journal of Immunology* **193**, 5294–5305 (2014).
61. Perez-Riverol, Y. *et al.* The PRIDE database at 20 years: 2025 update. *Nucleic Acids Res* gkae1011 (2024) doi:10.1093/nar/gkae1011.
62. de Boer, J. *et al.* Transgenic mice with hematopoietic and lymphoid specific expression of Cre. *Eur J Immunol* **33**, 314–325 (2003).
63. Poncet, N. *et al.* The catalytic subunit of the system L1 amino acid transporter (slc7a5) facilitates nutrient signalling in mouse skeletal muscle. *PLoS One* **9**, e89547 (2014).
64. Sinclair, L. V., Neyens, D., Ramsay, G., Taylor, P. M. & Cantrell, D. A. Single cell analysis of kynurenine and System L amino acid transport in T cells. *Nat Commun* **9**, 1981 (2018).
65. Miller, R. G. The use and abuse of filipin to localize cholesterol in membranes. *Cell Biol Int Rep* **8**, 519–535 (1984).

66. Baker, C. P. *et al.* DIA label-free proteomic analysis of murine bone-marrow-derived macrophages. *STAR Protocols* **3**, 101725 (2022).
67. Molina-Gonzalez, I. *et al.* Astrocyte-oligodendrocyte interaction regulates central nervous system regeneration. *Nat Commun* **14**, 3372 (2023).
68. Sollberger, G., Brenes, A. J., Warner, J., Arthur, J. S. C. & Howden, A. J. M. Quantitative proteomics reveals tissue-specific, infection-induced and species-specific neutrophil protein signatures. *Sci Rep* **14**, 5966 (2024).
69. Tyanova, S. *et al.* The Perseus computational platform for comprehensive analysis of (prote)omics data. *Nat Methods* **13**, 731–740 (2016).
70. Benjamini, Y., Krieger, A. M. & Yekutieli, D. Adaptive linear step-up procedures that control the false discovery rate. *Biometrika* **93**, 491–507 (2006).
71. The Gene Ontology knowledgebase in 2023 - PubMed. https://pubmed.ncbi.nlm.nih.gov/36866529/.
72. Kanehisa, M., Sato, Y., Kawashima, M., Furumichi, M. & Tanabe, M. KEGG as a reference resource for gene and protein annotation. *Nucleic Acids Res* **44**, D457-462 (2016).
73. Sherman, B. T. *et al.* DAVID: a web server for functional enrichment analysis and functional annotation of gene lists (2021 update). *Nucleic Acids Res* **50**, W216–W221 (2022).

Figure 1

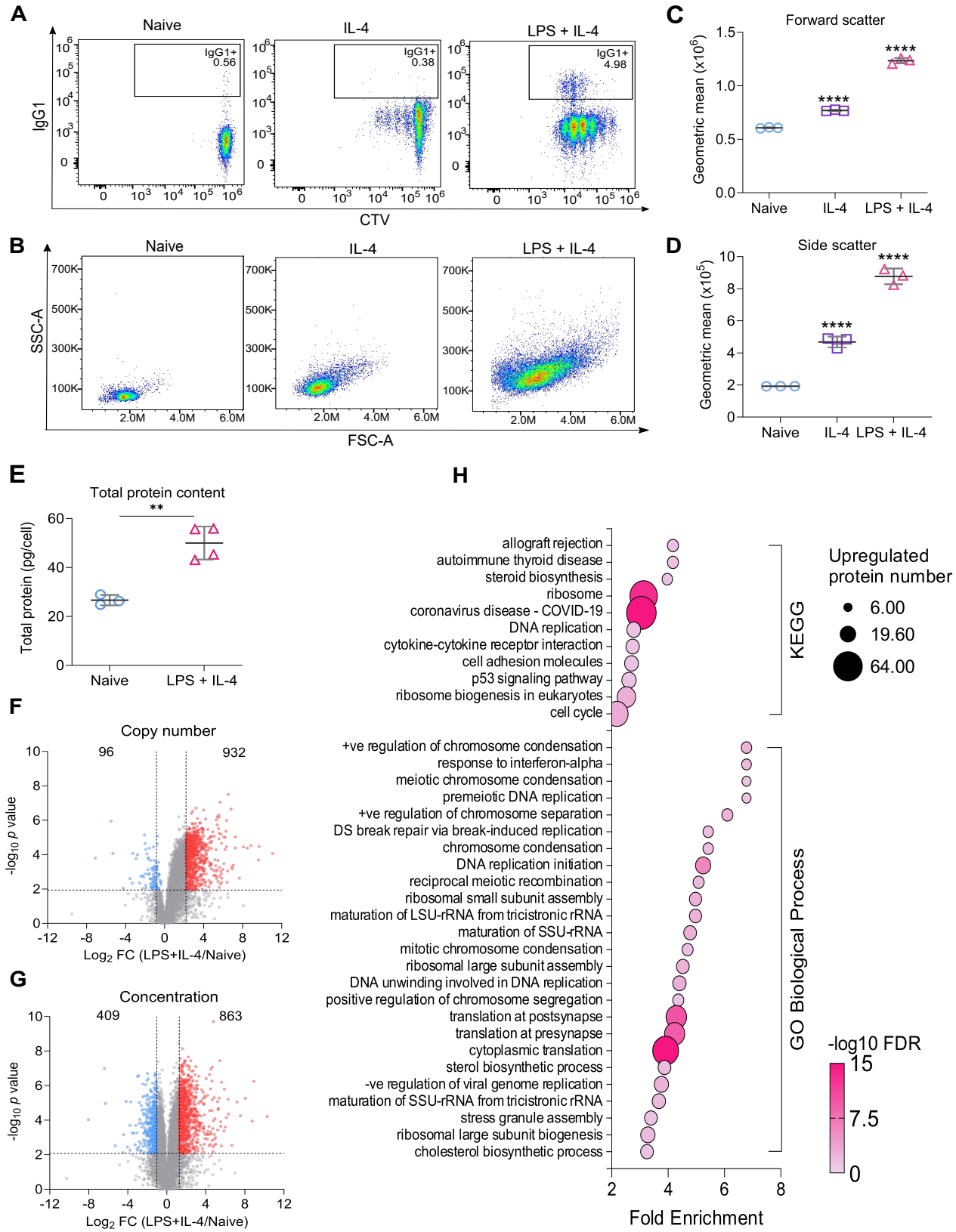

Figure 1. Stimulation with LPS + IL-4 promotes B cell proliferation and class switch recombination

(A-D) Lymph node cells were stained with Cell Trace Violet (CTV) and cultured in the presence of IL-4 (10ng/ml) or/and LPS (20μg/ml) for 72 hours and analysed by flow cytometry. Live CD19+ve B cells were identified using the gating strategy described in Figure S1A. **(A)** Representative flow cytometry plots comparing IgG1 expression and Cell Trace Violet (CTV) staining after 72 hours of IL-4 or LPS + IL-4 stimulation. **(B)** Representative plots for FSC and SSC at 72 hours of IL-4 or LPS + IL-4 stimulation with geometric means for the **(C)** forward scatter and **(D)** side scatter.

(E-H) Naïve B cells or B cells stimulated with LPS + IL-4 for 24 hours analysed by proteomics as described in the methods. n = 3 biologically independent samples for naïve cells and n = 4 biologically independent samples for LPS + IL-4 conditions. **(E)** Total protein content (pg/cell) was estimated from the proteomic data. **(F)** Volcano plot depicting changes in protein copy number in naïve vs LPS + IL-4 stimulated B cells. **(G)** Volcano plot showing the estimated cellular protein concentration (μM) in naïve vs LPS + IL-4 stimulated B cells. Horizontal dashed lines indicate q < 0.05. Vertical dashed lines indicate log2 fold change more than one standard deviation away from the median. **(H)** Enrichment analysis of the upregulated proteins in (G) against GO-term and KEGG databases.

Data is representative of three biological replicates **(A-D)**.

For **C-D**, p values were determined using one-way ANOVA followed by multiple comparison testing via Dunnett's analysis. For comparison to naïve B cells, **** indicates p<0.0001. For **E**, p values were determined using an unpaired T test (two-tailed) where ** indicates p<0.01. Refer to Table S3 for full statistics.

Figure 2

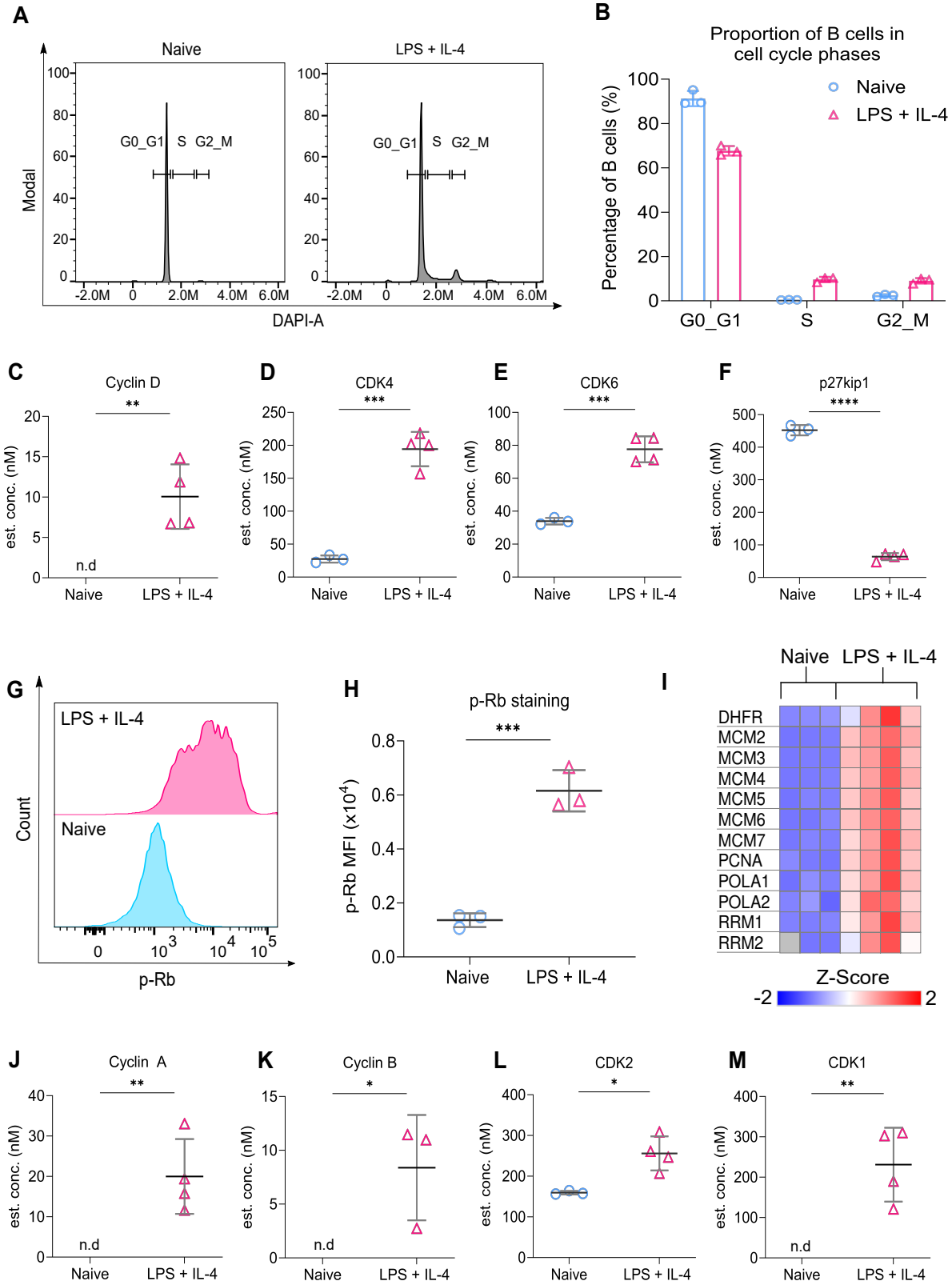

Figure 2. Proteins involved in cell cycle progression are upregulated in LPS + IL-4 activated B cells

(A-B) B cells were isolated from spleens and cultured in the presence of LPS (20µg/ml) and IL-4 (10ng/ml) for 24 hours before fixing and staining with DAPI. Gating strategy for DAPI staining in Figure S6B. **(A)** Representative histogram showing the proportion of cells in different phases of the cell cycle in the naïve and LPS + IL-4 stimulated B cells are shown with quantification of 3 technical replicates in **(B)**.

(C-F) Levels of **(C)** Cyclin D. **(D)**CDK4. **(E)** CDK6. **(F)** p27Kip1. Determined from the proteomic dataset described in Figure 1.

(G, H) B cells were isolated from spleens and cultured in the presence of LPS (20µg/ml) IL-4 (10ng/ml) for 24 hours before fixing and staining for phospho-retinoblastoma (p-Rb). Gating strategy for p-Rb staining in Figure S6B. **(G)** Representative histogram comparing p-Rb staining in naïve and LPS + IL-4 stimulated B cells and quantification of the MFI of 3 technical replicates in **(H)**.

(I) Heat map showing the expression of genes encoding for proteins involved in the cell cycle derived from the proteomic data.
Graphs depicting changes in cellular concentration (nM) of proteins implicated in cell cycle progression. Cyclin A **(J)**, Cyclin B **(K)**, CDK2 **(L)**, CDK2 **(M)**, determined from the proteomic dataset described in Figure 1.

Data is representative of two independent experiments **(A-B, G-H)**.
Statistical power was determined using an unpaired T test (two-tailed), where *p<0.05 for **K** and **L**, **p<0.01 for **C, J,M** ***p<0.001 for **D,E,H**, ****p<0.0001 for **F**.
Refer to Table S3 for full statistics.

Figure 3

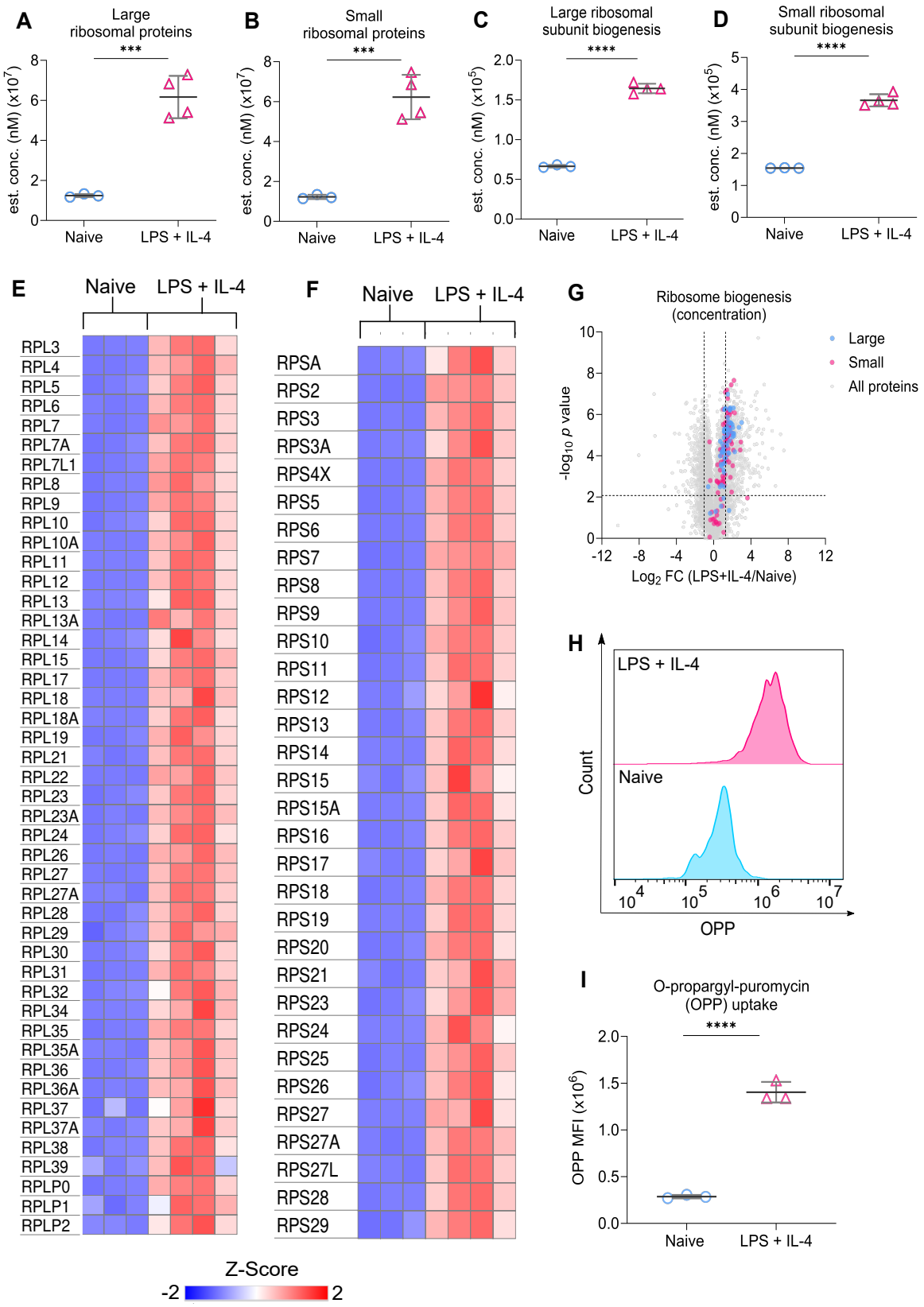

Figure 3. LPS + IL-4 stimulation promotes protein synthesis

(A-D) Graphs depicting changes in cellular concentration (nM) of the sum of proteins that make up ribosomal subunits or involved in ribosomal subunit biogenesis. **(A)** Large ribosomal proteins. **(B)** Small ribosomal proteins. **(C)** Large ribosomal subunit biogenesis. **(D)** Small ribosomal subunit biogenesis. Determined from the proteomic dataset described in Figure 1.

(E-F) Heat maps showing the expression of genes encoding for proteins that make up the **(E)** Large ribosomal subunit. **(F)** Small ribosomal subunit.

(G) Volcano plot showing the cellular protein concentration (μM) of proteins involved in large and small ribosomal subunit biogenesis between naïve vs LPS + IL-4 stimulated B cells. Horizontal dashed lines indicate q < 0.05. Vertical dashed lines indicate log2 fold change more than one standard deviation away from the median.

(H-I) Splenocytes were isolated and cultured in the presence of LPS (20μg/ml) IL-4 (10ng/ml) for 24 hours before fixing and staining for the uptake of puromycin analog O-propargyl-puromycin (OPP) to measure protein synthesis. Gating strategy for p-Rb staining in Figure S6C. **(H)** Representative histogram comparing OPP uptake in naïve and LPS + IL-4 stimulated B cells and **(I)** quantification of the MFI of 3 technical replicates in and is representative of one independent experiment.

Statistical power was determined using an unpaired t-test (two-tailed) where ***p<0.001 for **A** and **B**, ****p<0.0001 for **C, D,I.** Refer to Table S3 for full statistics.

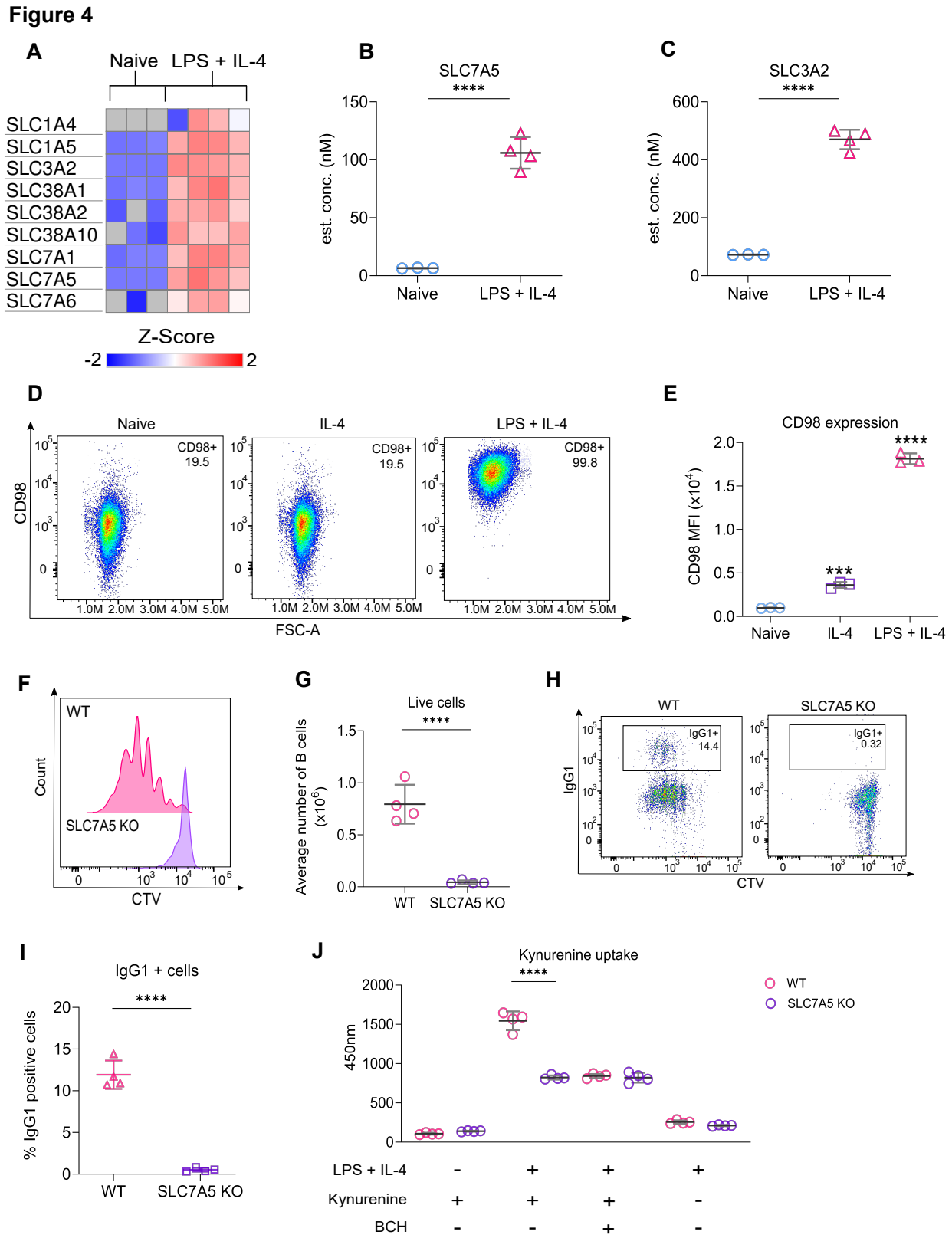

Figure 4. Amino acid transporter SLC7A5 is required for key B cell functions

(A) Heat map showing the expression of genes encoding for proteins involved in amino acid transport determined from the proteomic dataset described in Figure 1. **(B-C)** Graphs depicting changes in cellular concentration (nM) of the protein subunits that make up the amino acid transporter Lat1: **(B)** SLC7A5. **(C)** SLC3A2. **(D-E)** Lymph node cells were cultured in the presence of LPS (20μg/ml) and IL-4 (10ng/ml) for 24 hours before staining for CD98. **(D)** Representative FACS plot comparing CD98 expression and **(E)** quantification of the MFI of 3 technical replicates.

(F-I) B cells were isolated from the spleens of Wild-type (WT) and Slc7a5 fl/fl/Vav-iCre+/- (SLC7A5 KO) and stained with CTV prior to stimulation with LPS (20μg/ml) and IL-4 (10ng/ml) for 72 hours. **(F)** Histogram representing CTV staining of B WT and SLC7A5 KO B cells. **(G)** Live B cell number of WT and SLC7A5 KO mice. **(H)** Representative FACS plots comparing IgG1 expression and CTV staining of WT and SLC7A5 KO B cells. **(I)** Percentage of B cells that are IgG1+ in WT and SLC7A5 KO mice.
(J) B cells were isolated from spleens of WT and SLC7A5 KO mice and cultured with LPS (20μg/ml) IL-4 (10ng/ml) for 24 hours before fixing and staining for the uptake of kynurenine to measure amino acid uptake. **(J)** Quantification of kynurenine MFI between B cells from WT and SLC7A5 KO mice with (+) or without (-) LPS + IL-4, aminobicyclo-(2,2,1)-heptane-2-carboxylic acid (BCH) or EBSS.

(F-J) Data is representative of one independent experiment with 4 biological replicates for WT and 4 biological replicates for Slc7a5 fl/fl/Vav-iCre+/-.
(D-E) Data is representative of two independent experiments.

Statistical power was determined using an unpaired t-test (two-tailed) where ****p<0.0001 for **B, C, G, I**.
For **(E)** statistical power was determined using one-way ANOVA followed by multiple comparison testing via Dunnett's analysis where **** indicates p<0.0001.
For **(J)** statistical power was determined for using two-way ANOVA followed by multiple comparison testing via Tukey HSD analysis, where ****p<0.0001. Refer to Table S3 for full statistics.

Figure 5

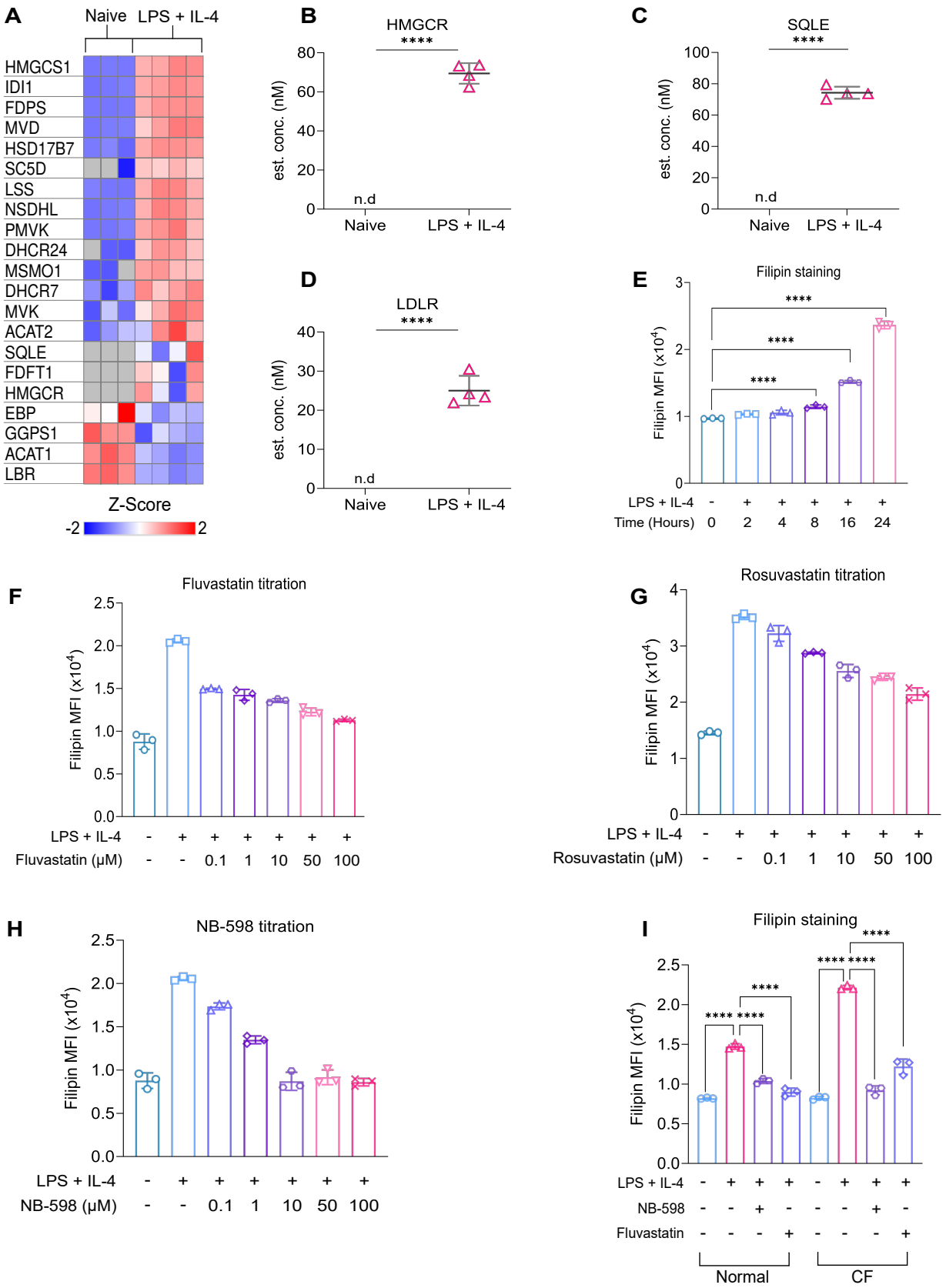

Figure 5. LPS + IL-4 stimulation upregulates cholesterol metabolism in B cells

(A) Heat map showing the expression of genes encoding for proteins involved in cholesterol metabolism.

(B-D) Graphs representing changes in cellular protein concentration (nM) of **(B)** HMGCR. **(C)** SQLE. **(D)** LDLR.

(E) Splenocytes were isolated, plated in cholesterol free media and cultured in the presence of LPS (20μg/ml) and IL-4 (10ng/ml). The cells were fixed at the stated time points and staining with filipin before acquisition. **(E)** Filipin staining timecourse.

(F-H) Same as **(E)** but cells were pre-treated with varying concentrations of NB-598, Fluvastatin or Rosuvastatin for 45 minutes prior to stimulation. **(F)** Fluvastatin titration. **(G)** Rosuvastatin titration. **(H)** NB-598 titration.

Same as **(F-H)** but the cells were plated in normal or cholesterol free media. **(I)** Filipin staining after 24 hours of Fluvastatin or NB-598 treatment.

Data is representative of one **(E)**, two **(F-H)** or three **(I)** independent experiments.
Statistical power was determined using an unpaired t-test (two-tailed) where ****p<0.0001 for **B, C,D**.
Statistical power for **(E)** was determined using a one-way ANOVA followed by multiple comparison testing via Dunnett's analysis, for comparison to naïve B cells, **** indicates p<0.0001.

Figure 6

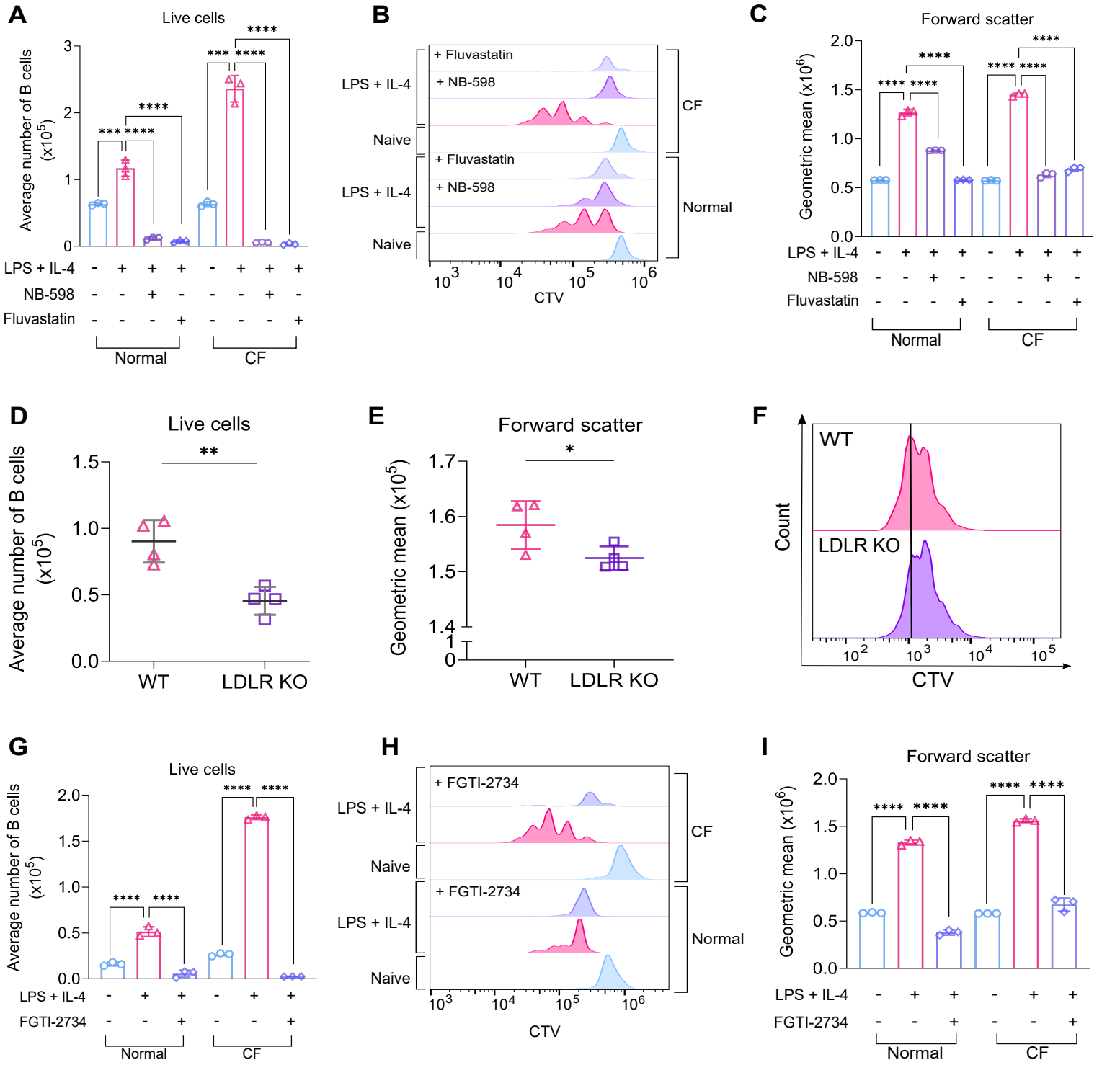

Figure 6. Blocking rate-limiting enzymes in the cholesterol biosynthesis pathway reduces B cell growth, survival and proliferation

(A-C) B cells were isolated from spleens and cultured in normal or cholesterol free media. The cells were stained with CTV, then pre-treated with or without Fluvastatin (50μM) or NB-598 (10μM) for 45 minutes prior to stimulation with LPS (20μg/ml) and IL-4 (10μg/ml) for 48 hours. **(A)** Live B cell number after NB-598 or Fluvastatin treatment. **(B)** Histogram representing CTV staining following NB-598 or Fluvastatin treatment. **(C)** Forward scatter of B cells following NB-598 or Fluvastatin treatment.

(D-F) Splenocytes were isolated from wild-type (WT) and Ldlr-/- mice (LDLR KO) and cultured in normal media. The cells were stained with CTV prior to stimulation with LPS (20μg/ml) and IL-4 (10μg/ml) for 48 hours. **(D)** Live B cell number between WT and LDLR KO mice. **(E)** Forward scatter of B cells between WT and LDLR KO mice. **(F)** Histogram representing CTV staining between WT and LDLR KO mice. Data is representative of 2 independent experiments using 4 biological replicates for WT and 4 biological replicates for LDLR KO each time.

(G-I) Same as A-C but with pretreatment using FGTI-2734 (10μM) **(G)** Live B cells number after FGTI-2734 treatment. **(H)** Histogram representing CTV staining following FGTI-2734 treatment. **(I)** Forward scatter of B cells following FGTI-2734 treatment.

Data is representative of three independent experiments for **(A-C, G-I)**.

Statistical power was determined using two-way ANOVA followed by multiple comparison testing via Tukey HSD analysis, where **** indicates p<0.0001. Refer to Table S3 for full statistics.

Figure 7

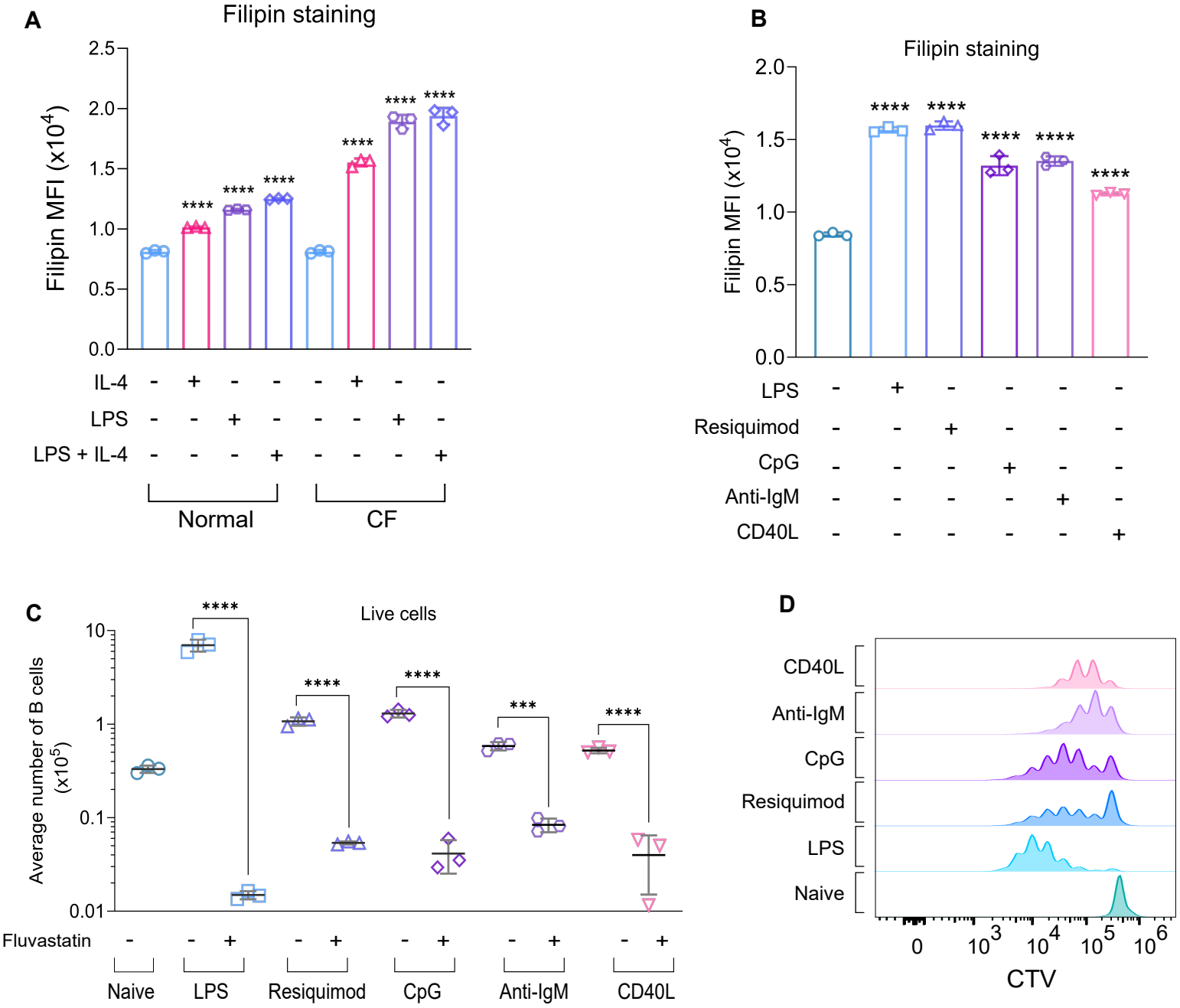

Figure 7. Cholesterol is required for the growth and proliferation of B cells regardless of stimuli

(A) Splenocytes were isolated and plated in normal media, prior to stimulation with LPS (20μg/ml) and/or IL-4 (10μg/ml). The cells were fixed after 24 hours and stained with filipin. **(A)** Measurement of cellular cholesterol content by filipin staining.

(B) Splenocytes were isolated and plated in normal media prior to stimulation with LPS (20μg/ml), Resiquimod (10μg/ml), ODN 1826 (1μg/ml), Anti-IgM (10μg/ml), or CD40L (500ng/ml). The cells were fixed after 24 hours and stained with filipin. **(B)** Measurement of cellular cholesterol content by filipin staining after 24 hours of stimulation.

(C-D) B cells were isolated from spleens and cultured in normal media. The cells were stained with CTV, then pre-treated with or without Fluvastatin (50μM) for 45 minutes prior to stimulation with LPS (20μg/ml), Resiquimod (10μg/ml), ODN 1826 (1μg/ml), Anti-IgM (10μg/ml), or CD40L (500ng/ml) for 48 hours. **(C)** Live B cell number after Fluvastatin treatment. **(D)** Histogram representing CTV staining following stimulation.

Data is representative of two independent experiments for **A-D**.

For **(A)** statistical power was determined using one-way ANOVA followed by multiple comparison testing via Sidak's analysis, where **** indicates $p<0.0001$.
For **(B)** statistical power was determined using one-way ANOVA followed by multiple comparison testing via Dunnett's test where **** indicates $p<0.0001$.
For **(C)** statistical power was determined using two-way ANOVA followed by multiple comparison testing via Sidak's analysis, where **** indicates $p<0.0001$.

Refer to Table S3 for full statistics.